

# An Integrated Geomechanical Investigation, Multi-Parameter Monitoring and Analyses of Babadağ-Gündoğdu Creep-like Landslide

Halil Kumsar<sup>1</sup> · Ömer Aydan<sup>2</sup> · Hisataka Tano<sup>3</sup> · Sefer Beran Çelik<sup>1</sup> · Reşat Ulusay<sup>4</sup>

Received: 28 February 2015 / Accepted: 19 August 2015 / Published online: 1 September 2015  
© Springer-Verlag Wien 2015

**Abstract** A creep-like landslide in the Gündoğdu district of Babadağ town in Denizli (Turkey), where about 2000 people lived within the damaged houses, has been moving with a velocity of 4–14 cm/year since 1940s. Field observations and monitoring together with geomechanical laboratory tests were carried out to investigate the causative factors of the landslide. These studies were conducted as a part of an international research project performed by Turkish and Japanese scientists since 2000. Long-term monitoring stations established involved measurements of meteorological parameters, displacements, acoustic emission counts, variations in groundwater table, borehole strain measurement, in situ permeability and infiltration characteristics of the slope forming materials, and vibrations induced by weaving machines during their operation. Geomechanical properties of the sandstone and marl, which form the unstable slope, were determined from laboratory tests. In addition to the use of conventional 2-D equilibrium method of analyses, a new approach for modelling the long-term creep-like behaviour of the landslide body, based on discrete finite element method, was also proposed and used to analyse the landslide. It was found that the sliding mass has been involving several

zones of weakness (interface) between the sandstone and marl layers through in situ monitoring. The monitoring data of pipe strain, groundwater level fluctuation and rainfall, and AE data showed that slope movement accelerated during and after rainy seasons. It was obtained that the proposed numerical method based on discrete finite element method (DFEM), which considers the softening and hardening of stiffness of the weakness zone as a function of rainfall and, is capable of simulating creep-like behaviour of the landslide. Disaster and Emergency Management Authority of Turkey also considered the results of this research and the landslide area was designated as a Natural Disaster Area and the people living in the unstable part of the town were re-settled at a new area.

**Keywords** Creep-like landslide · Babadağ · Multi-parameter monitoring · Discrete finite element · Natural hazard

## 1 Introduction

Slope failures may be caused as a result of various triggering factors such as geological conditions, topography, physical and mechanical properties of discontinuities, geomechanical features of geo-materials forming the slope, groundwater, dynamic forces from natural and artificial sources and surface loading. A typical slope stability analysis includes identification of factors causing slope failure, failure mode, mathematical modelling and/or physical modelling for stability assessment and monitoring of slope response.

Most of the slope stability studies do not integrate geomechanical investigations and testing, monitoring and stability analyses. If there is a settlement to be affected by

✉ Halil Kumsar  
hkumsar@pau.edu.tr

<sup>1</sup> Department of Geological Engineering, Pamukkale University, Kınıklı, Denizli, Turkey

<sup>2</sup> Department of Civil Engineering and Architecture, University of the Ryukyus, Nishihara, Okinawa, Japan

<sup>3</sup> Department of Civil Engineering, Nihon University, Koriyama, Japan

<sup>4</sup> Department of Geological Engineering, Hacettepe University, Beytepe, 06800 Ankara, Turkey

slope instability, the issue becomes more complex and involves additional social measures for people living in such areas. Particularly, moving people from such areas to other safer places requires a lot of efforts in convincing people and authorities for such an action. Today, particularly due to increasing population, migration from small settlements to towns and cities has resulted in increasing demand on land use and forced the people to settle on hilly grounds. As a result of this, urban and rural development has taken place over the years on or adjacent to landslides. In some cases, it can be possible to apply remedial measures against threatening landslides to stabilise them. But in some cases, where the movement spans over a long time and threatens the life and structures, huge amount of cost for remedial works may be needed and the people living at such places under high risk must be evacuated.

Babadağ town of Denizli, which is located in western Turkey (Fig. 1a) and founded on a hilly ground, is one of

the oldest settlements where the textile industry is very popular. The Gündoğdu district of the town is under the threat of a creep-like landslide (Fig. 1b) for more than 70 years and this instability resulted in a high risk for about 2000 people living in this part of the town. In this study, this landslide was investigated by using field measurements, in situ geotechnical tests, laboratory geomechanical tests on slope forming materials and their discontinuities, multi-parameter monitoring techniques, stability analysis based on conventional limiting equilibrium methods and modified discrete finite element method (DFEM), which was described in this study, and the mechanism of the instability and contributing factors to the movement were presented. This paper also presents a unique case history to implement the integrated study of geomechanical investigations, laboratory and in situ tests, continuous multi-parameter monitoring and analytical and numerical analyses into practice in saving life of about 2000 people living in

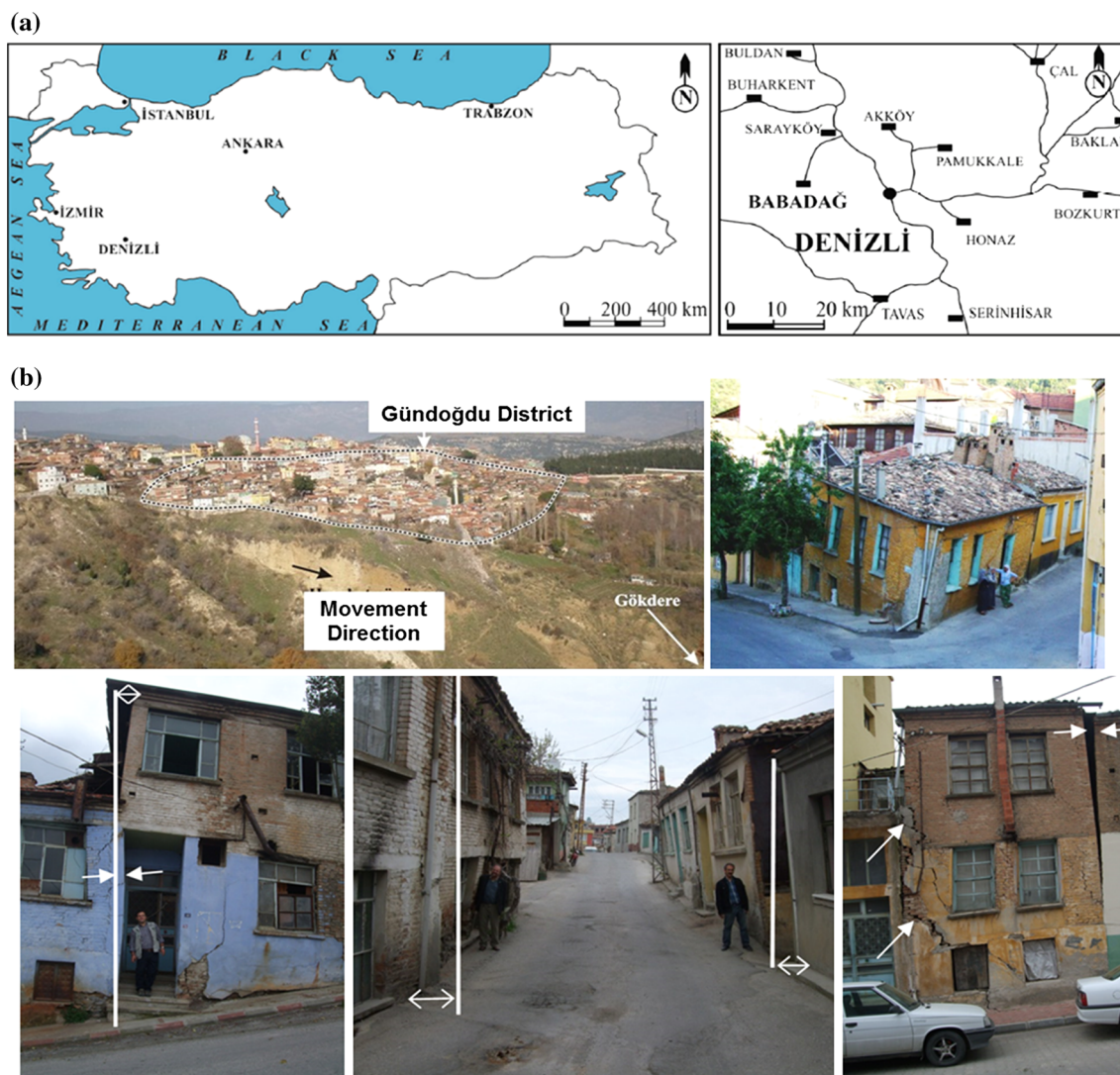


**Fig. 1** a Location map of Babadağ town, b views from the unstable Gündoğdu district and some damaged houses

an active creep-like landslide area before a disastrous event which may be caused due to continuous heavy rainfalls and/or an earthquake with a magnitude larger than 6 in the close vicinity of Babadağ town.

## 2 History of the Babadağ Gündoğdu Landslide

A creep-like landslide affecting the life of about 2000 local people living in the Gündoğdu district of Babadağ town has been continuing for more than 70 years at least (Fig. 1b). The landslide was first reported by Önay (1946). Since then this part of the town has been moving toward the valley of Gökdere Stream (to E–SE) flowing from south to north at the east of Babadağ (Fig. 1b). The other districts of the town founded on metamorphic rocks have not been affected by any slope movement. The Gündoğdu district was then designated as a natural disaster area. A fire in Babadağ occurred in 1948 and 26 houses were burned out and the authorities decided to resettle the people in Göveçlik town, but the people of Babadağ did not accept to move (i.e. Özpinar et al. 1999a; Tano et al. 2008). Ergün (1969) reported that Mareşal Fevzi Çakmak, Atatürk and Gündoğdu districts were located in a potential landslide area. Therefore, it was suggested that the people living in these districts including those, whose houses were burned during the 1948 fire, should move to a safer place near the Temlik location in Sarayköy town 15 km NE of Babadağ. However, the people remained to live in the Gündoğdu district.

Özpinar et al. (1999a), based on their preliminary site observations, classified the type of slope failures observed in the vicinity of Babadağ town as mudflow, talus flow, planar, circular and composite types of sliding failure. Özpinar et al. (1999b) also indicated that the factors affecting Gündoğdu landslide were mainly groundwater, topography, erosion at the toe of the slope, sewage and drinking water infiltration into the slope from broken pipes and sewage channels, surface loading imposed by the structures on the ground.

Due to the slope movements, which have been still continuing, the local people living in the Gündoğdu district have been negatively affected. Some selected damages on the structures in the Gündoğdu district resulted from the creep-like landslide are shown in Fig. 1b.

## 3 Geology and Seismotectonics of Babadağ and Its Close Vicinity

In Babadağ and its surroundings, the Paleozoic–Mesozoic-aged metamorphic rocks form the bedrock, which are unconformably overlain by the Cenozoic-aged sedimentary rocks. The bedrock, called Ortaköy formation (Öngür

1971), is mainly composed of mica schist, mica and quartz schist, graphite schist, garnet schist, amphibolite schist and occasionally marble. It extends towards higher altitudes at the south (Fig. 2) and southern part of Babadağ town is located on the schists of this formation. In the study area, Cenozoic sedimentary rocks are represented by the Kolonkaya formation which consists of four members called Ahıllı marl, Babadağ sandstone-marl, Manastır conglomerate and Mollaahmetler conglomerate (Şimşek 1984). The youngest sedimentary sequence in the study area is the Pliyo-Quaternary-aged Kelleci conglomerate member of the Asartepe formation (Fig. 2).

Babadag town partly settles on the Babadağ sandstone-marl member and is surrounded by Ahıllı marl member from its north and west (Fig. 2). The Ahıllı marl member mainly consists of cream and white coloured marl and claystone with occasional limestone layers. The Babadağ sandstone-marl member conformably overlaying the Ahıllı marl member is observed in the town centre and in the Gündoğdu landslide area and consists of the alternation of light yellowish marl and sandstone. The sandstone layers are very weak and include sands of metamorphic origin, which are mainly micas. Their thicknesses vary from a few mm to 15 cm (Fig. 3).

The Manastır sandstone member, cropping out at the west of Babadağ (Fig. 2), is composed of yellowish-red conglomerate and sandstone succession. The thickness of this member is less than 100 m (Öngür 1971). The Kelleci conglomerate, which unconformably overlays the Kolonkaya formation and extends in approximately E–W direction in the east of Babadağ, has an alluvial origin and is represented by conglomerate, sandstone and siltstone alternations (Fig. 2).

Babadag is located in the Büyük Menderes Graben of the West Anatolian Fault System of Turkey and the Babadağ horst consists of listric normal faults dipping towards north as seen in Fig. 2. The Babadağ fault, one of the faults in the site, forms the boundary between the metamorphic basement rocks and Cenozoic-aged formations, and passes approximately through the middle of Babadağ town. Where it runs towards east in SE direction, the fault forms the boundary between the Quaternary and metamorphic basement and due to this, the fault is considered as an active fault (Şaroğlu et al. 1992).

The Denizli basin is one of the most seismically active regions of Turkey (Ergin et al. 1967; Eyidogan et al. 1991; Aydan et al. 1996a; Aydan 1997). The seismicity of the Denizli basin is divided into two broad groups, namely, historical seismicity and instrumental seismicity. Some antique cities in Denizli Province, Karacasu (Aydın Province), Büyük Menderes and Küçük Menderes basins were repeatedly destroyed by historical strong earthquakes (Aydan and Kumsar 2005, 2014). Therefore, it is most

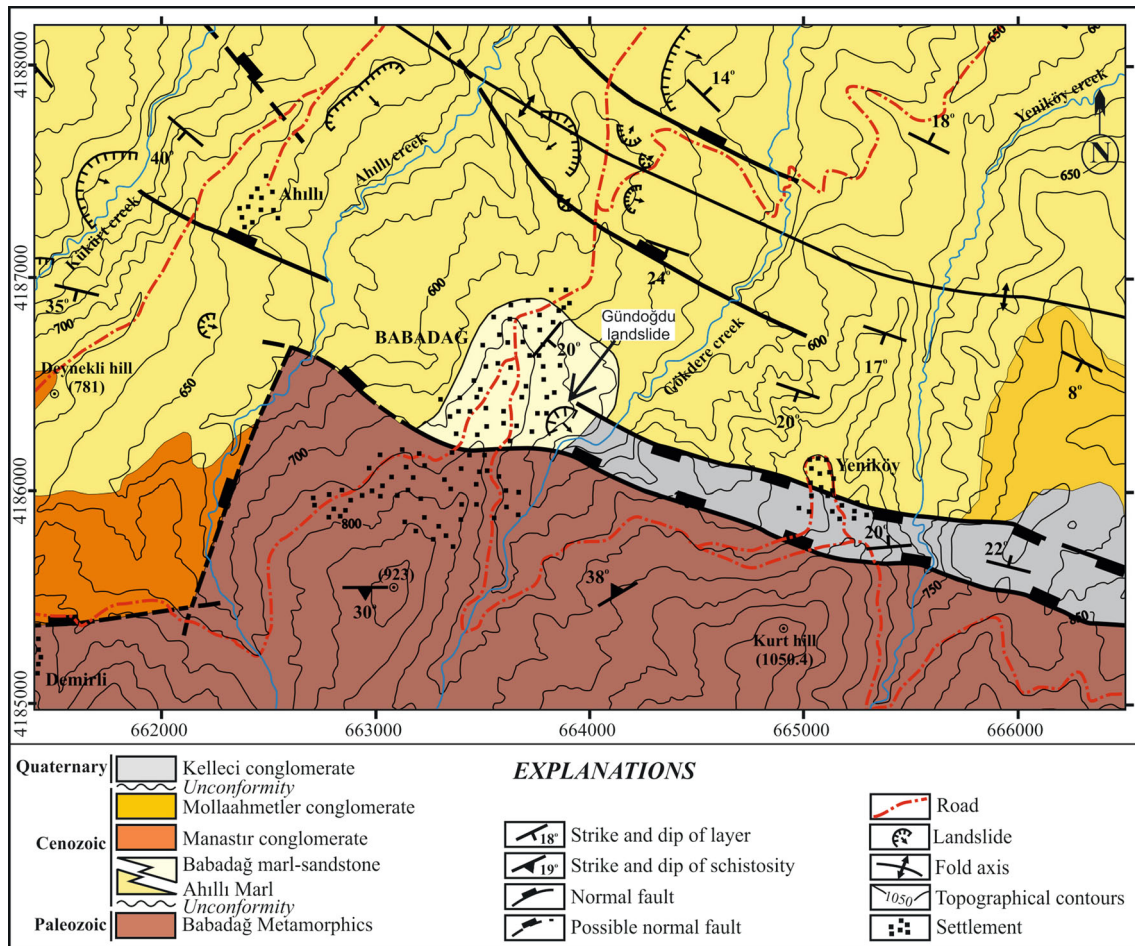


**Fig. 2** Geological map of Babadağ and its close vicinity (modified from Çevik 2003 and Hañer 2013)

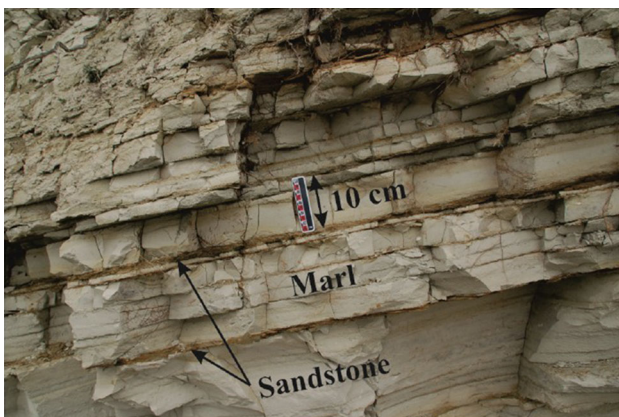


**Fig. 3** A view from the Babadağ sandstone-marl member in the south of Babadağ town centre

likely that the region can produce very large earthquakes in due time (Kumsar and Aydan 2007). Earthquakes and their relation to the active faults in Denizli basin between 1900 and 2014 are shown in Fig. 4. The magnitudes of the

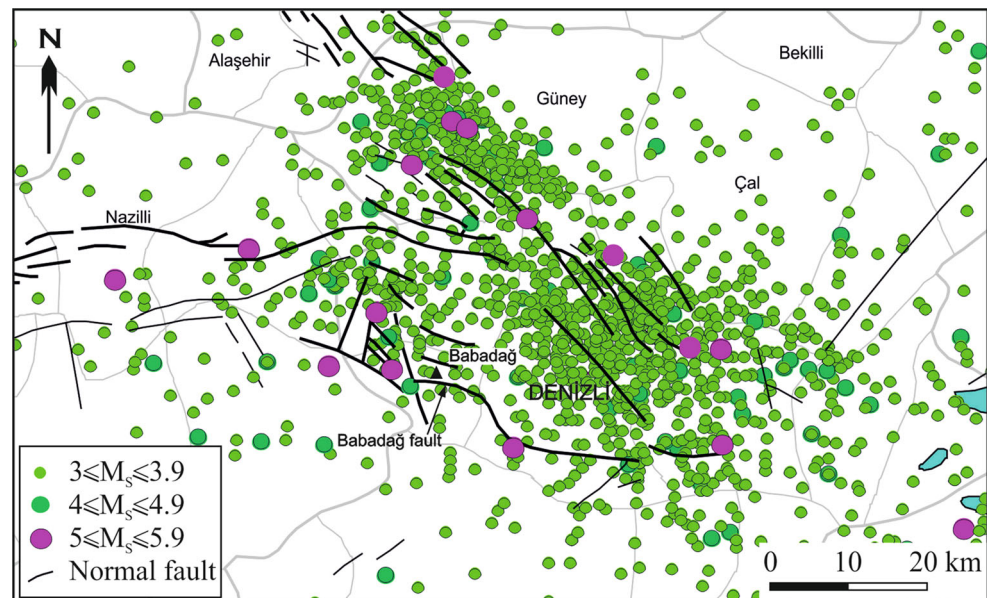
earthquakes are less than 6.0 and their epicentres are located along the active fault zones in the basin (Kumsar et al. 2008). In addition, based on the assessments by Aydan et al. (2002), possible future earthquakes with magnitudes of about 6 can be expected in this region, which takes place in the 1st degree earthquake zone according to the Earthquake Zonation Map of Turkey.

## 4 Measurements and Monitoring Studies for the Assessment of the Landslide Mechanism and Affecting Factors

### 4.1 Vibration Measurements Induced by Weaving Machines in the Town

The main income of the people living in Babadağ is from the production of linen textile using their weaving machines in their houses. There were about 1500 weaving machines in Babadağ before 2005. In situ acceleration measurements were performed during the machines were

**Fig. 4** Seismicity in Denizli basin between 1900 and 2014 (MTA 2014; KOERI 2014)



in operation in order to investigate their dynamic effects on the slope failure (Fig. 5). Dynamic effects of wooden and metal weaving machines were investigated by operating them in the following three combinations (Aydan et al. 2003).

Case 1: Two metal weaving machines were operated in c2 atelier

Case 2: Four weaving machines were operated in a2 and b2 ateliers

Case 3: All of the weaving machines were operated in a2, b2 and c2 ateliers

Acceleration measurements were taken in N–S, E–W and up–down directions simultaneously. Acceleration measurements in Case 1 and Case 2 yielded similar results. Amplitudes of accelerations measured near to the weaving machines ranged between 20 and 25 gals and the acceleration values were higher near the weaving machines and they decreased with distance (Fig. 5). Amplitudes of the accelerations for Case 3 were less than 25 gals. The maximum acceleration next to one wooden frame weaving machine is 50 gals, while single metal weaving machine induces acceleration up to 25 gals. It is also noted that the wooden frame weaving machines induced accelerations 3–4 times greater than those generated by the metal weaving machines.

#### 4.2 In situ Permeability and Infiltration Measurements

In order to assess the hydrogeological conditions of the study site and their effects on the slope instability, in situ permeability and infiltration tests were performed within the sandstone–marl alternation in the unstable part of Babadağ.

Ten falling head tests were performed in two holes and the permeability coefficients were computed using the measured responses of time vs. water head decrease according to Barron et al. (1970)'s equation and back analysis using the finite element code (FEM) developed by Aydan (1998). The results show that the permeability coefficient of the sandstone–marl succession varies between  $6.686 \times 10^{-4}$  and  $1.250 \times 10^{-3}$  cm/s from the Barron et al. (1970)'s equation and  $7.640 \times 10^{-4}$  and  $1.356 \times 10^{-3}$  cm/s based on the back-analyses (Table 1). It was concluded that since the permeability coefficient of the marl is considerably lower than that of the sandstone, water percolates through the fractures in the marl and porous sandstone.

Two infiltration tests were performed in borehole SK3 using a water pressure tensor. During the tests, the first and second arrivals of water were observed after 600 and 1380 s, respectively (Fig. 6). The infiltration velocity values calculated between 1.67 and 1.85 mm/sec imply that water head variations in Gündoğdu district may quickly develop soon after the rainfalls in Babadağ and play an important role in the variation of the rate of slope movement.

#### 4.3 Deformation Measurements by Aerial Photogrammetry

In this study, long-term ground deformation of a landslide through the use of aerial photogrammetry technique was first time applied to Gündoğdu district of Babadağ town (Fig. 7a). The aerial photogrammetry was used to obtain ground strain which was computed by using an interpolation technique of finite element method (Atak et al. 2003). A series of aerial photographs of Babadağ and its close

**Fig. 5** Acceleration measurement induced by weaving machines: **a** instrumentation layout, **b** view of a metal weaving machine, **c**–**d** acceleration measurement results (Aydan et al. 2003)

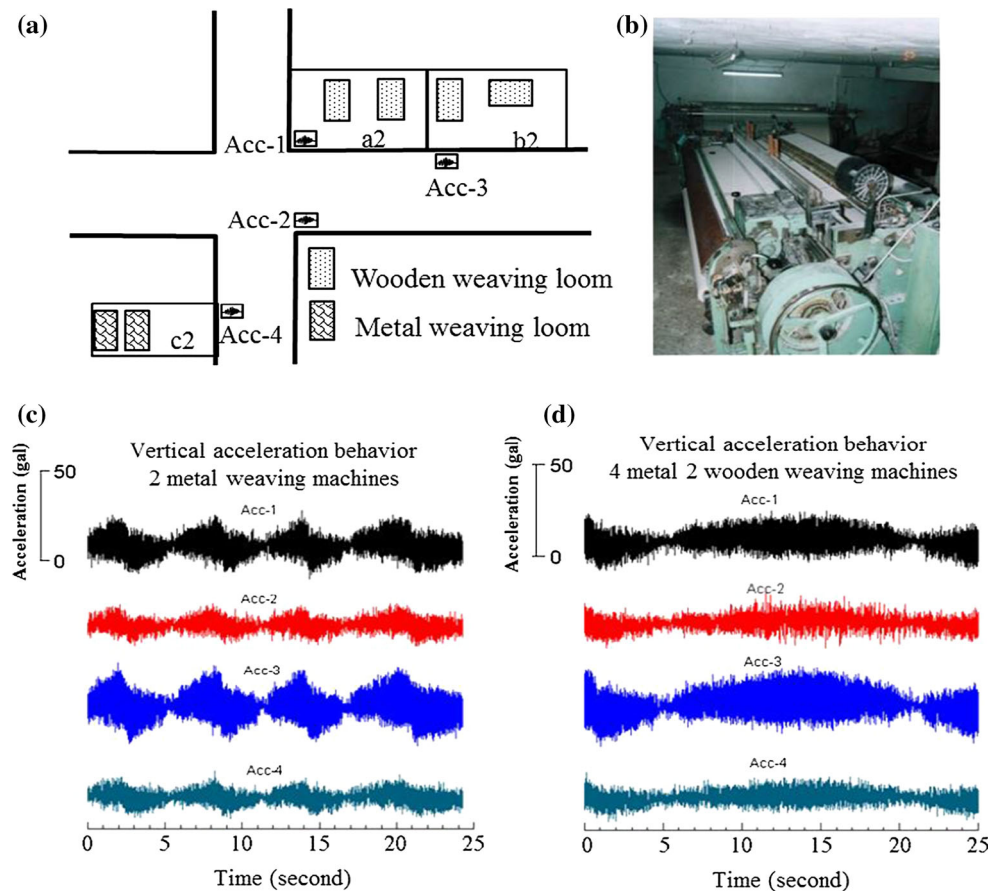


**Table 1** Inferred permeability coefficients of tests in the Gündoğdu district

Test no.	Permeability coefficient (cm/s) (Barron et al. (1970)'s formula)	Permeability coefficient (cm/s) (FEM)
Test 1–1	$5.482 \times 10^{-4}$	$6.815 \times 10^{-4}$
Test 1–2	$1.250 \times 10^{-3}$	$1.356 \times 10^{-3}$
Test 2–1	$3.523 \times 10^{-4}$	$2.521 \times 10^{-4}$
Test 2–2	$5.000 \times 10^{-4}$	$6.560 \times 10^{-4}$
Test 3–1	$3.584 \times 10^{-4}$	$2.568 \times 10^{-4}$
Test 3–2	$5.701 \times 10^{-4}$	$7.640 \times 10^{-4}$
Test 4–1	$3.523 \times 10^{-4}$	$2.503 \times 10^{-4}$
Test 4–2	$4.710 \times 10^{-4}$	$4.936 \times 10^{-4}$
Test 5	$4.727 \times 10^{-4}$	$4.831 \times 10^{-4}$
Test 6	$6.686 \times 10^{-4}$	$4.942 \times 10^{-4}$

vicinity taken by the General Command of Mapping of Turkey between 1960 and 2001 (1960, 1972, 1988, 1993 and 2001) were used to determine ground deformations for a period of 41 years. The base mesh of the area is shown in Fig. 7b.

Figure 7c, d shows that the deformation rate of the Gündoğdu district is quite high between 1988 and 1993 and

it seems increased when compared to the other date intervals of the measurement (Fig. 8a). The computed tensile strains (Fig. 8a) are consistent with ground cracks and damages of the houses in the Gündoğdu district. Some compressive and tensile strains are developed within the landslide area that tends to rotate clockwise (Fig. 8b) (Atak et al. 2003; Kumsar et al. 2004; Tano et al. 2006a). Although the deformation is within the accelerated creep stage, general tendency of the points 12 and 29 is alarming. The overall deformation rate ranges between 40 mm/year and 160 mm/year which are quite consistent with the deformation measurements discussed in Sect. 4.4.1.

#### 4.4 Multi-parameter Monitoring System for the Gündoğdu Landslide

A multi-parameter in situ monitoring system, which consists of relative displacement measurements on structures along the boundary between stable and unstable regions, groundwater level variation in two boreholes, pipe strain measurement in one borehole, acoustic emission (AE) counts at four different locations, gap measurement in one location, and measurement of meteorological parameters, was established in the town (Fig. 9).

#### 4.4.1 Relative Displacement Monitoring System

The relative displacements were obtained from the variation of distances between structures on stable and unstable parts of the town along the perimeter of the unstable area using a laser metre (weight: 800 g, allowable distance: 0.3–40 m, accuracy of distance: 1.5 mm, size: 5 × 8 × 20 cm). The points located in the stable and unstable parts of the town are called base and target points,

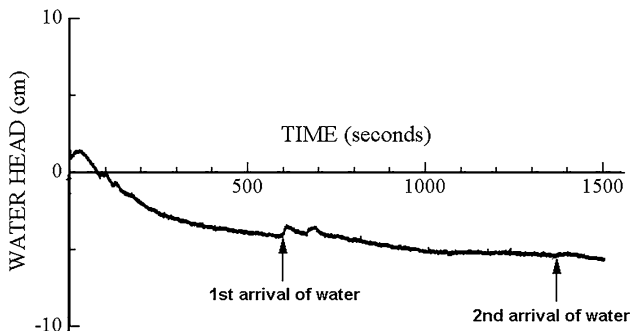


Fig. 6 Water head variations with time in infiltration test 1

respectively (Fig. 10), and three target points were marked at each base point.

The ground surface of Babadağ is covered by different pavement materials, and therefore, direct observations on the ground surface are difficult. The measurements by laser metre were taken at 30 locations (Fig. 10) between a base point to three target points, which were marked with water-resistant painting and fixed to a metal plate. Sometimes these points were destroyed by humans mistakenly due to renovation works for the houses. The measurements were taken between 2005 and 2012 at six-month intervals (Kumsar et al. 2004).

#### 4.4.2 Meteorological Records and Groundwater Monitoring

A meteorological station was installed in the garden of Directorate of Babadağ Agricultural Works Department in order to investigate the effect of rainfall on the landslide in Babadağ. Precipitation, humidity, outside temperature and ground temperature at depths of 1, 0.75, 0.50 and 0.25 m below the ground surface were automatically recorded at 1 h interval.

Fig. 7 Measured velocity vectors and computed principal strain rates for 1960–2001 (Atak et al. 2003): **a** aerial view of Babadağ, **b** the base mesh of the area, **c** calculated deformation vectors, **d** calculated principal strain rates

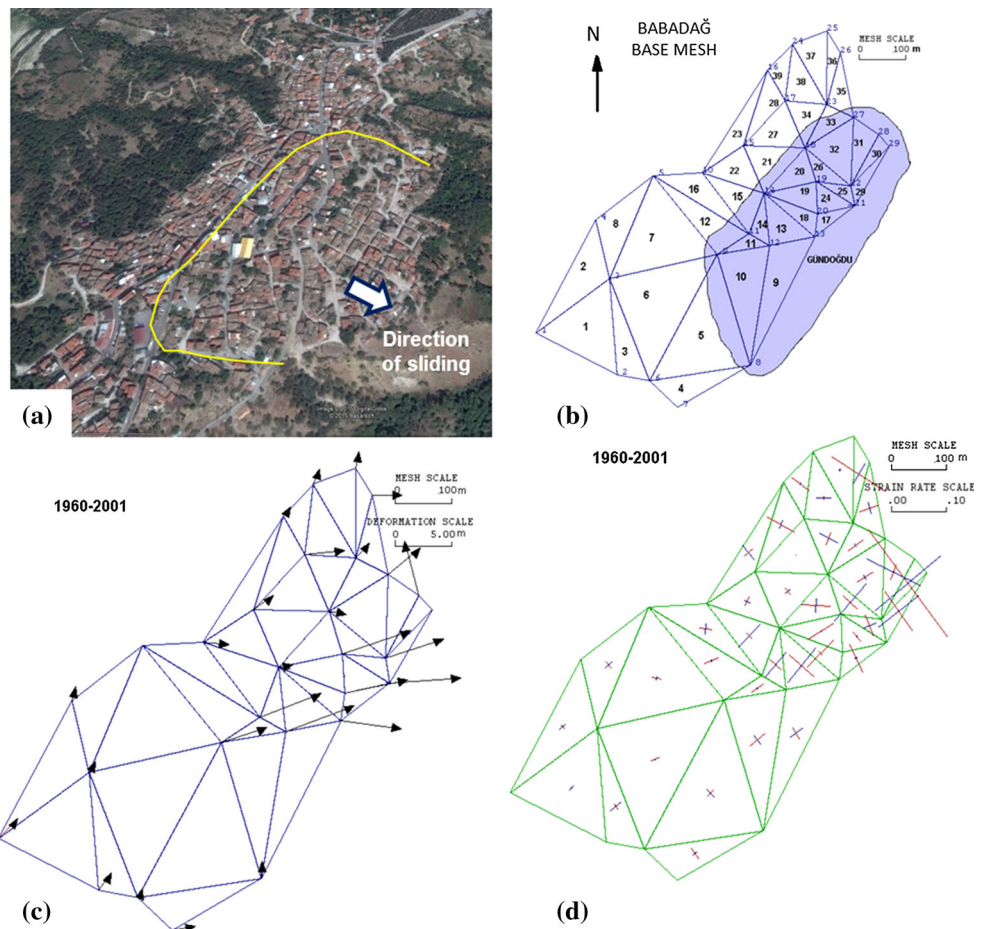


**Fig. 8** **a** The absolute horizontal displacement of some selected points, **b** tensile strain rates of some selected elements

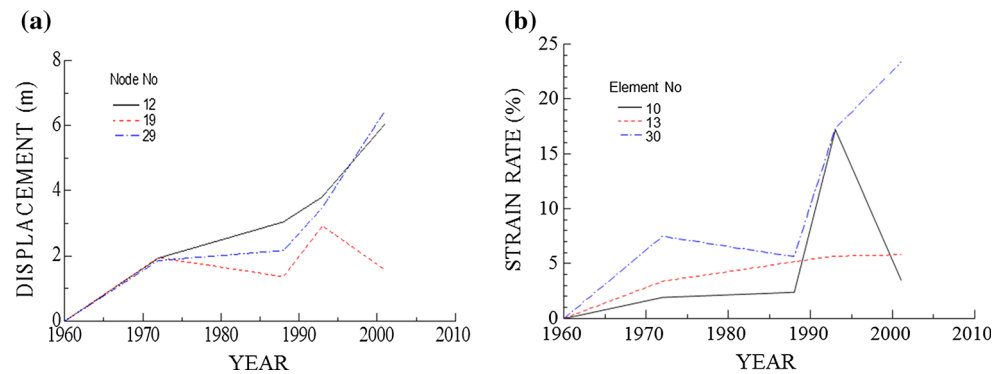
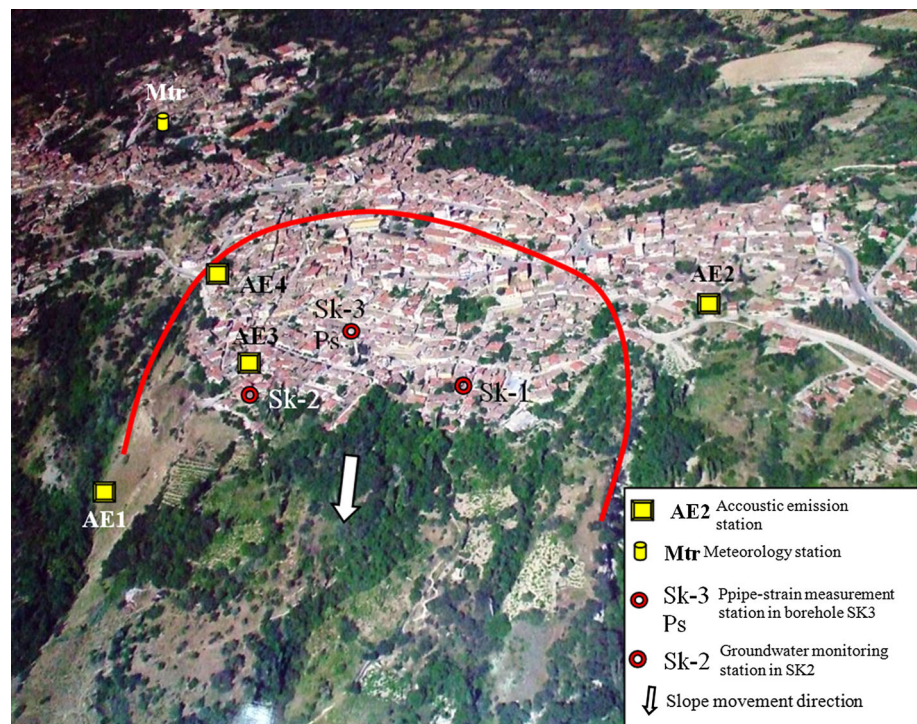


**Fig. 9** Multi-parameter monitoring system established for the Gündoğdu landslide



Three deep boreholes (SK1, SK2 and SK3) with a depth of 55 m were drilled in the Gündoğdu district to monitor the groundwater level variations at 1 h intervals. In borehole SK1, the groundwater level was deeper than 55 m, and therefore, could not be monitored. The groundwater level was measured in borehole SK2 in which an automatic groundwater measuring and recording system was installed. Additional data, from the three new boreholes (SK 5, 6, 7) drilled at the northern stable part of the town, were also monitored using a dipmeter between 2005 and 2006.

#### 4.4.3 Acoustic Emission Monitoring System

Ultrasonic elastic waves caused by fracture or slippage of materials are called as acoustic emission (AE). Therefore, such a signal of wave is expected to be caused by the

movements of a landslide body (Tano et al. 2003). The Acoustic Emission Counting System (NUAECS) of Nihon University, which was used in this study, consists of three main components as shown in Fig. 11a. The AE measuring system (Fig. 11b–e) operates with battery and records the data for 400 days. The logger records a pulse count associated with AE waves exceeding a threshold value (15 mV). The active sensor is directly attached onto a rock or a wave guide, which is installed at 1 m depth inside the slope, while a dummy sensor is suspended (Fig. 11f). If an AE count is recorded by the active and dummy sensors simultaneously, the active count is cancelled from the record (Tano et al. 2003, 2008; Kumsar et al. 2004). In this study, four AE monitoring stations were established in the Gündoğdu district. First one (AE1) is located in the toe area of the slope where failure surfaces were observed



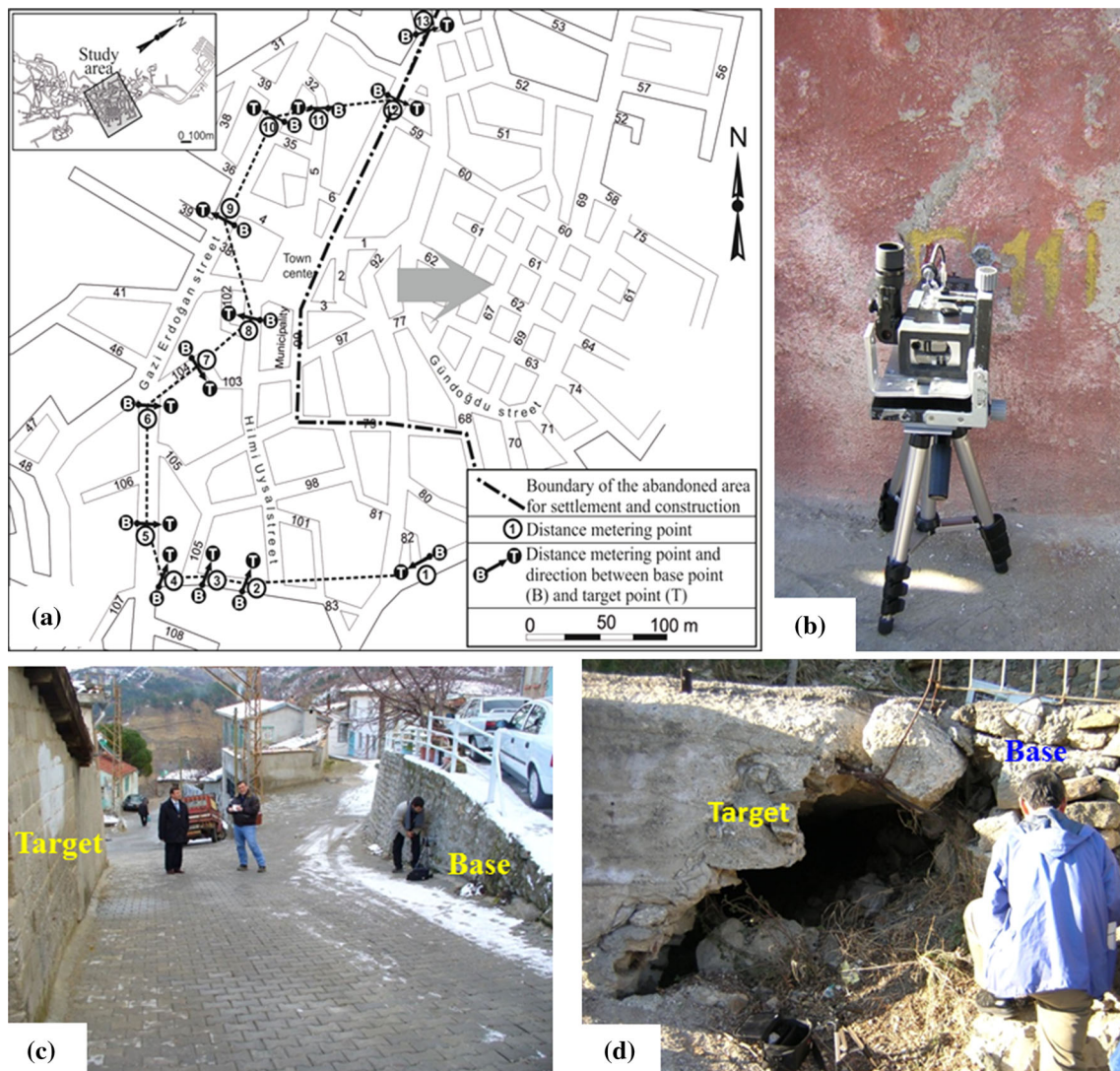


**Fig. 10** Layout of the relative displacement measurement system in the Gündoğdu landslide area

(Fig. 11b, c, d). AE2 station is located in the stable part of the Gündoğdu landslide area where sandstone-marl succession is seen clearly on a steep cliff (Fig. 12a), AE3 station was installed next to the damaged house in the unstable area (Fig. 12b). AE4 station was installed at the boundary of the landslide (Fig. 12c), where AE and relative displacement measurement systems were established (Fig. 12d).

#### 4.4.4 Borehole Pipe Strain Measurement

Pipe strainmeters have been commonly used in slope monitoring projects in Japan as they are cheaper than extensometers. As borehole SK3 was filled up with the sands of Babadağ sandstone-marl succession up to 10 m deep from the ground surface (Tano et al. 2006b), a 50 m deep new borehole (SK4) was drilled at a distance of 10 m

far from borehole SK3 in the unstable area of the Gündoğdu landslide (Fig. 13a)

Strain gauges, attached to the inner surface of plastic pipes, were lowered into the borehole (Fig. 13b) and the connection cable of each strain gauge was connected to the data logger in the safety box on the top of the borehole (Fig. 13c). At every 2 m interval, two sets of strain gauges ( $\epsilon_{x1}$ ,  $\epsilon_{x2}$ ) and ( $\epsilon_{y1}$ ,  $\epsilon_{y2}$ ) were attached to a plastic pipe to measure the axial strain on the inner surface of the pipe. Two sets are mutually perpendicular to each other. When bending occurs in the pipe, one of the gauges has positive sign, while the other one has negative sign (Fig. 13d). These time strain gauges were set up such that all strain would indicate positive straining. From these measurements, it would be possible to determine the direction of sliding. The y-axis was adjusted to be parallel to the sliding direction nearby borehole SK4. The channel number of the

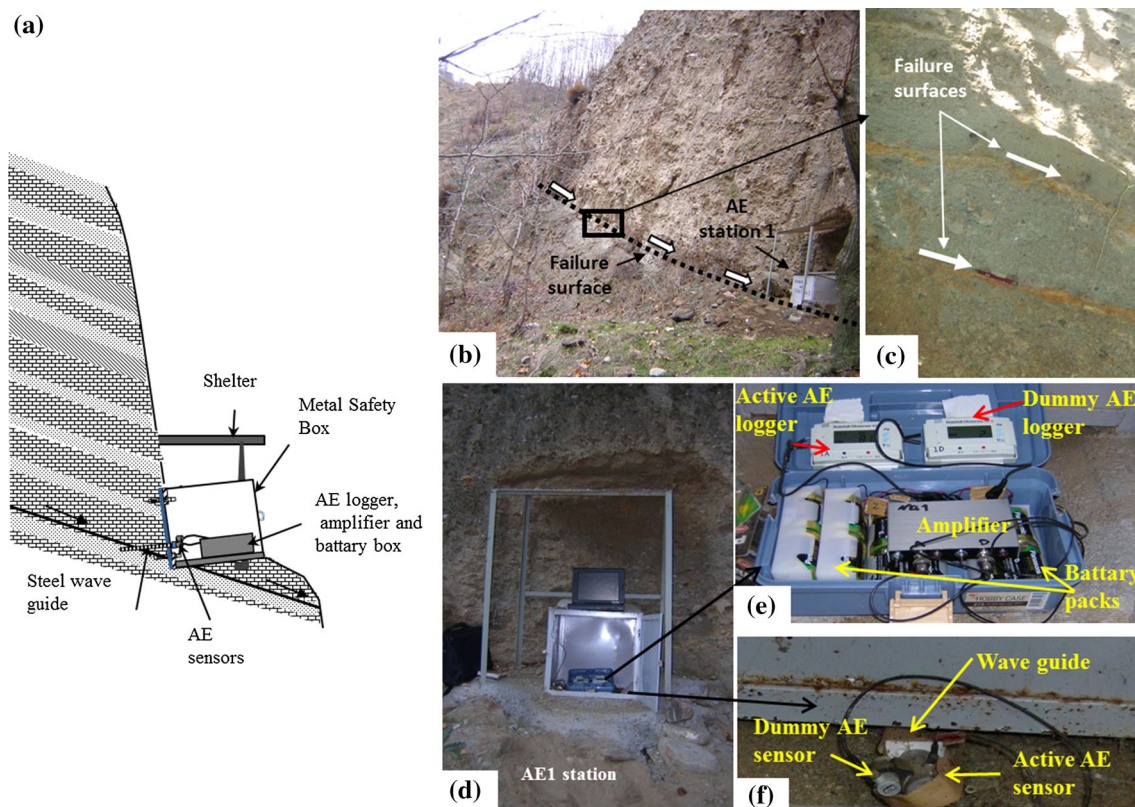


**Fig. 11** a An illustration of the in situ acoustic emission (AE) measuring system used in this study (modified after Tano et al. 2006a), b location and measuring system of AE1 station at the toe of

the Gündoğdu landslide, c failure surfaces observed at AE1 location, d power supply, loggers and amplifiers of AE1 station, e active and dummy AE sensors and wave guide of AE1 station

logger restrained the number of measurement points. The strains at 15 levels with a 2 m interval for a total length of 30 m could be measured. The first part of 17.6 m long section from the top was non-instrumented. Therefore, it could be possible to measure the ground straining up to a depth of 49.6 m from the top of the borehole.

## 5 Evaluation of Measurements and Monitored Data

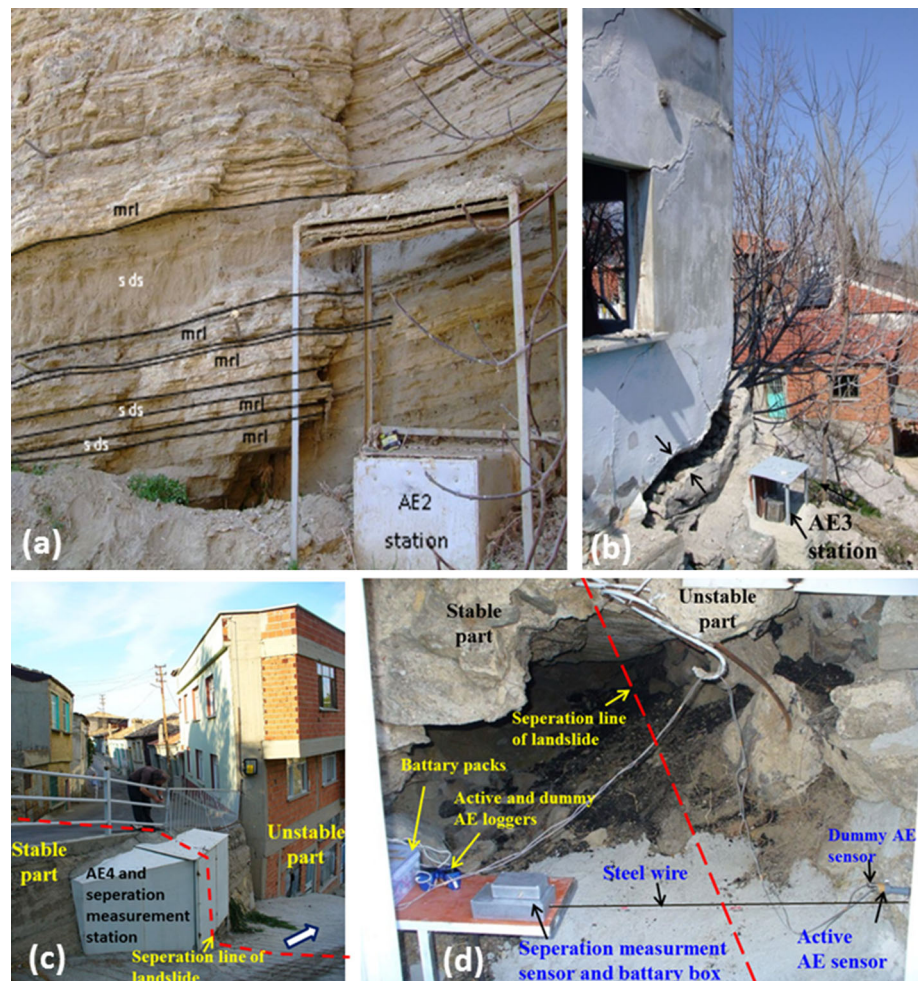
The field measurements and monitored data since 2001 were evaluated and discussed by the authors in several publications (Aydan 2003; Çevik 2003; Çevik and Ulusay 2003, 2005; Kumsar et al. 2004, 2012; Tano et al. 2003, 2006a, b, 2008; Çelik 2012). In this section, the results of the field measurements and the monitored data are compiled and evaluated.

There was a decrease in groundwater level from 27 to 31.5 m below the ground surface in borehole SK2 between 2002 and 2011. Meteorological data presented in Fig. 14 shows that there is a decrease of annual rainfall from 798 to 378 mm between 2002 and 2008, respectively. This is consistent with the groundwater measurement in borehole

SK2. However, there is a large increase in rainfall in 2009 with a total amount of 1243.5 mm, while it decreased to 794.5 mm in 2010. In addition, the data from the three additional boreholes (SK5, 6, 7) also indicated that the groundwater raised up to shallow depths at the end of winter seasons and confirmed the assessments of the data from the previously drilled boreholes.

The evaluation of the relative displacement measurements at the boundary between the stable and unstable parts in the Gündoğdu could not fully be carried out during the monitoring period due to the renovation and/or repair of the houses in the district between 2005 and 2012 is shown in Fig. 15. There is a divergence at stations 1, 2, 3, 4/1 and 4/2 between 2005 and 2008. The maximum divergence of 180 mm was measured at Station 1 where there was a separation crack at the boundary. In the same period, Station 8 had a 50 mm convergence. This implies that there was a backward tilting of the buildings at this locality. Stations 2, 7, 9 and 11 were monitored for a period of 7 years and the Station 2 had a 250 mm divergence, while the others had a divergence less than 20 mm (Fig. 15). As seen from the rainfall data, the separation of the landslide from the stable part of the slope increased under the influence of increasing rainfall in Babadağ (Fig. 15).

**Fig. 12** **a** AE2 station and sandstone (sds)-marl (mrl) succession, **b** AE3 station and structural damages, **c** location of AE4 station, **d** active and dummy sensors, loggers and battery pack of AE4 station



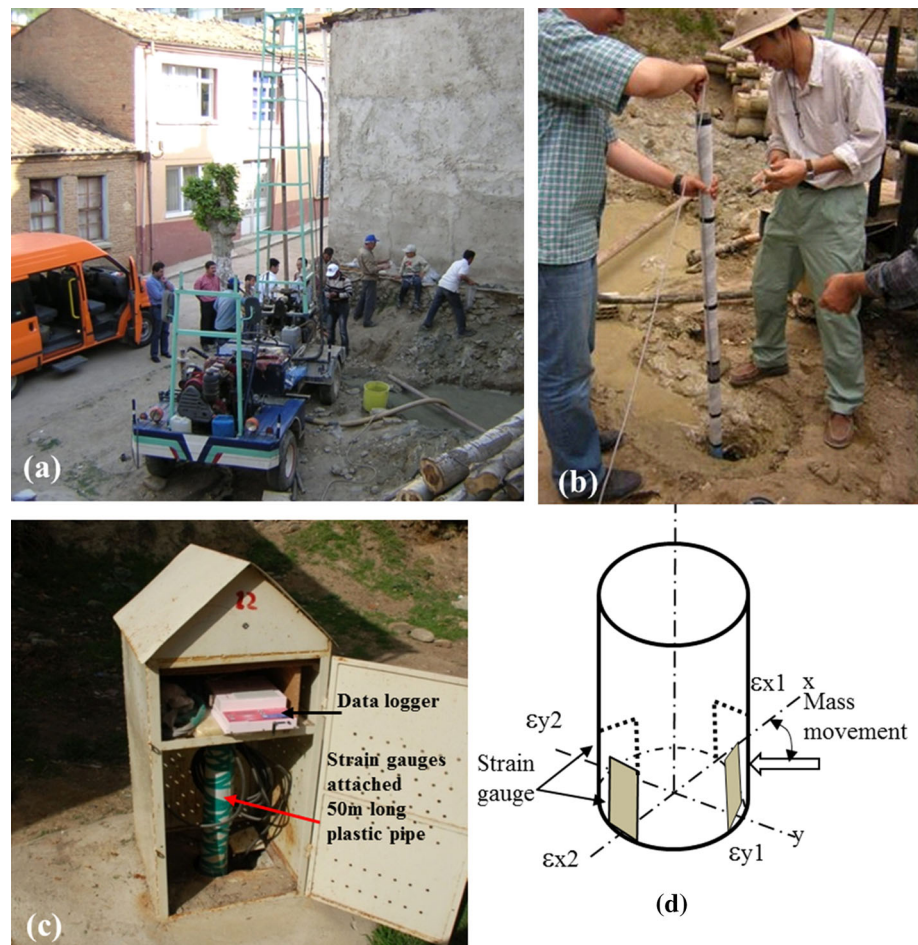
Since Station 1 is located at the boundary line between the unstable and the stable parts (next to Station AE4, see Fig. 12c), a gap measurement system was set up and measurements were taken at an interval of 1 h. At this station, AE measurement station AE4 was set up on 31 August 2007. The station, which was covered by a metal safety box, was distorted and damaged throughout the monitoring period between 2007 and 2012. 6 and 10 cm of horizontal and vertical separations, respectively, were observed at this station.

The relation between rainfalls, AE measurements and relative displacements are shown in Fig. 16. There is an increase in divergence between the stable and unstable parts of the slope at the location of station AE4 in autumn and winter seasons when rainfall increased. There is a convergence in spring season. The total numbers of the active AE counts increased distinctively throughout the monitoring period. This is because of the progressive displacement in the slope and traffic activity of the vehicles on the asphalt road just above the station AE4. The estimated convergence between the stable and unstable parts of the

slope was 20 mm between 24 September 2009 and 17 January 2012, but it was measured as 10 mm. This difference may have been resulted due to installation condition of the base point, on which the roller of the measuring steel wire was fixed.

The monitoring data, representing the period of monitoring between 06 August 2005 and 7 May 2009, from the pipe strain, groundwater level fluctuation, rainfall, AE1, AE2 and AE3 stations were compiled and shown in Fig. 17. As noted from the figure, there is a notable deformation at 9 and 18 m below the ground surface until 2 December 2007, while there is a decrease in the groundwater level below the ground surface from 30.5 to 31.25 m between 6 August 2005 and 24 September 2006. When a rainy season started at the end of September 2005, the groundwater level increased to 30.75 m below the ground surface. In this period, AE counts were observed mainly at stations AE1 and AE3, which are located in the active part of the landslide. Station AE2 is located in the stable part of the Gündoğdu region and the AE counts recorded at this station were mainly due to the fall of marl

**Fig. 13** **a** Drilling of 50 m deep borehole SK4, **b** installation of pipes on which strain gauges were attached, **c** view of the station after construction, **d** locations of the strain gauges attached on the plastic pipe (Tano et al. 2006a; Çelik 2012; Kumsar et al. 2012)



and sandstone blocks from the top of the cliff to the roof of the AE station.

Displacements at the levels of 15 and 36 m in the borehole SK4 started to increase during the period between 4 January 2007 and 2 December 2007. There were no data for the groundwater level measurement and rainfall between 13 February 2005 and 10 May 2005, and 20 June 2007 and 15 December 2007, respectively. During this period, the AE counts of AE1 station varied from 10 to 345 from 24 May 2007 to 6 February 2007, respectively. At Station AE3 also AE counts ranging between 10 and 270 were recorded during the measurement period. The AE counts recorded at Station AE2 were less than 75 since the station is located in the stable part of the slope.

During the period between 4 August 2008 and 7 May 2009, there was no significant deformation in the pipe strain data until the end of September 2008. In Babadağ and its vicinity, a rainy season started in October 2008 and lasted until the end of May 2009. During this period, distinct displacements developed at levels of 29 and 36 m of the borehole SK4 as seen in Fig. 17. The AE activities at the stations AE1 and AE3 were also remarkable as seen in

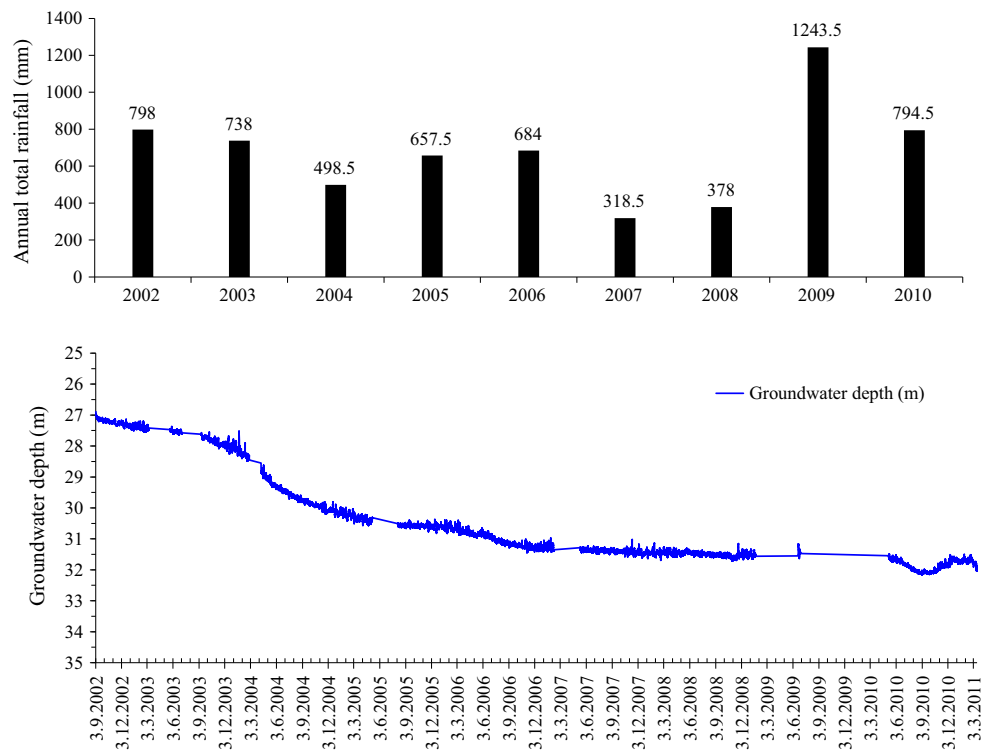
the same figure. The groundwater data were missed during this season due to a technical problem.

## 6 Geomechanical Properties of the Slope Forming Materials and Discontinuities

Different authors (Çevik 2003; Çevik and Ulusay 2005; Kumsar et al. 2004, 2015; Çelik 2012) determined geomechanical properties of the Babadağ sandstone-marl succession under different conditions and those of the discontinuities. The laboratory tests were conducted according to the methods suggested by ISRM (2007). Physical and mechanical properties of the sandstone and marl layers in the Babadağ member determined by Kumsar et al. (2004) are given in Table 2.

Two marl samples taken from Delikır area of Babadağ were tested in direct shear test with a shearing rate of 0.5 mm/min under consolidated and drained conditions. Their water contents range between 23 and 24 (%) but their shear strength is different from each other (Table 3). Cohesion of yellowish marl is higher than reddish marls (Kumsar et al. 2015).

**Fig. 14** Groundwater level fluctuations in borehole SK2 and rainfall in Babadağ realised between 2002 and 2011



The results of direct shear tests on the interface between the sandstone and marl, along which the instability occurs in Babadağ, under various shearing rates and drained conditions obtained by Çevik (2003) and Çevik and Ulusay (2005) and Çelik (2012) are given in Table 4. When the shearing rate is low, the interface has low shearing strength. The highest shearing strength was obtained at a shearing rate of 0.5 mm/min. Table 4 suggests that cohesion of the bedding planes (interface) is very low and can be ignored when residual strength is achieved.

In situ and laboratory tilt tests along the interfaces (bedding planes) between sandstone–sandstone, sandstone–marl and marl–marl layers under dry and saturated conditions were also performed and the results from these tests are given in Table 5. Friction angle under saturated conditions is sometimes larger than those determined under dry condition. This is thought to be suction produced by clayey nature of marl samples.

## 7 Assessment of Stability and Mechanism of the Gündoğdu Landslide

### 7.1 Analyses by the Conventional Limiting Equilibrium Method

As for preliminary analyses of stability, first the stability assessment of the Gündoğdu landslide was carried out

using conventional limiting equilibrium (LEM) techniques (i.e. Hoek and Bray 1981; Kumsar et al. 2000). However, it should be noted that this type analyses could not evaluate the creep-like behaviour of an unstable body. The failure surface was determined based on the results from the measurements taken by pipe strain deformation data, which indicate that large deformations were observed at 9, 15, 18, 29 and 36 metres below the ground surface in borehole SK3 located in the unstable area. The largest deformation was recorded at 29 m at the end of the monitoring period. The dip of the bedding planes in the Babadağ sandstone–marl ranges between 6° and 24° and particularly between 14° and 24° in the sliding area with a dip direction of 120° and 127° (SE) towards the stream (Çevik 2003; Çevik and Ulusay 2005; Çelik 2012; Kumsar et al. 2012). The mode of failure is planar as observed at the toe of the slope in the Gökdere Stream where AE1 monitoring station was installed (see Fig. 11b).

Topographic map of Babadağ (Fig. 18a) was digitised and loaded to SLOPAC2D software developed by Kumsar (1993) and a topographic cross section was constructed showing the failure surface (Fig. 18b) by using pipe strain and surface deformation monitoring data. The dip of the failure surface was determined as 17° to SE. On the basis of numerous direct shear tests on interfaces between sandstone and marl units under both dry and saturated conditions (Çelik 2012), the cohesion and friction angle based on linear Mohr–Coulomb failure criterion were

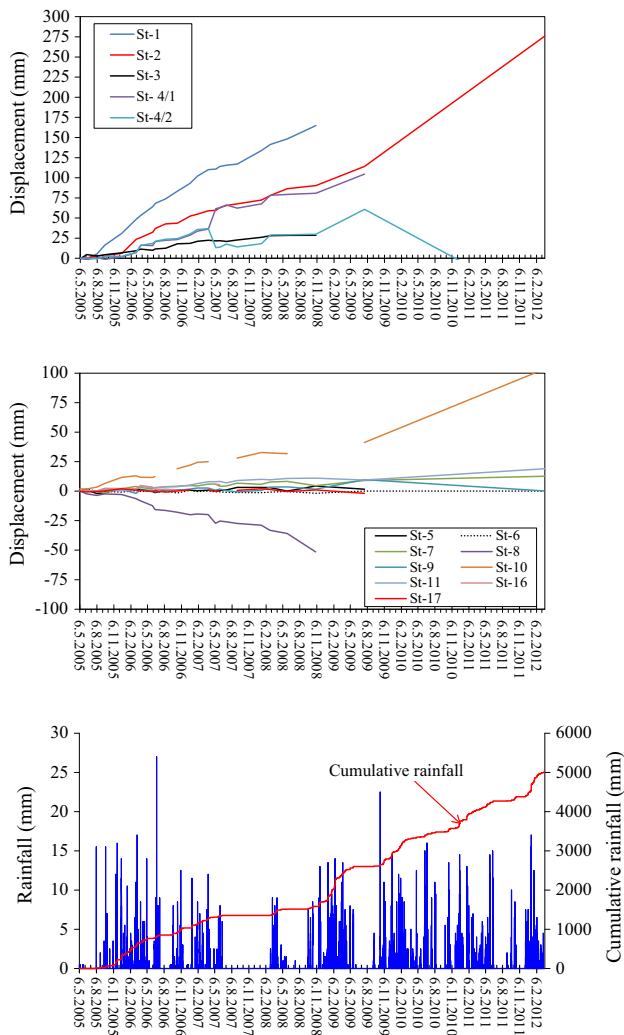


**Fig. 15** Relation between the relative displacement measurements and rainfall data

determined as 5 kPa and  $20^\circ$ , respectively. The average unit of the mass was determined as  $18.7 \text{ kN/m}^3$ . Groundwater profile was determined from the groundwater monitoring data of borehole SK2. Since the depth of the groundwater table varied from 27 to 31.5 m in 2002 and 2012, respectively, two groundwater profiles were used and effective stresses were calculated. The stability analysis of the slope was carried out by limiting equilibrium method (LEM) based on Coulomb's linear failure envelope and utilising the slice method for planar failures (i.e. Kumsar, 1993; Aydan et al. 1989, 1997). The factor of safety of the slope ranges between 1.17 and 1.28 for the chosen properties of the failure plane, unit weight of the unstable body and groundwater levels located at 27 and 31.5 m below the ground surface. Model experiments consisting of marl blocks with a size of  $40 \times 40 \times 10 \text{ cm}$  and a 10-mm-thick sandstone layer using the materials obtained from

Gündoğdu district for simulating planar sliding case with purely frictional resistance by Çelik (2012) and Çelik et al. (2011) showed that the sliding did not occur under dry conditions when the failure plane was inclined for the inclination angle of failure plane for  $17^\circ$ . It could only slide if the angle of failure plane angle was more than  $32^\circ$ , which implies the safety factor more than 2.19. The experimental results for wet interfaces of sandstone and marl were quite similar to those for dry case. Experiments under fully saturated condition could not be carried out as marl disintegrates when it is immersed in water. As marl absorbs water, marl gets softened and the interface between marl and sandstone layer is expected to be lower than those under wet conditions as given in Table 4 and reported by Çevik (2003) and Çevik and Ulusay (2005). However, the experiments by Çelik (2012) and Çelik et al. (2011) indicated higher strength values than those reported by Çevik (2003) and Çevik and Ulusay (2005) and given in Table 4.

Çevik and Ulusay (2005) also analysed the Gündoğdu landslide using the limit equilibrium method proposed by Hoek and Bray (1981) mentioned above and the upper, lower and mean values of shear strength properties given in Table 4 for groundwater table observed in the field and a groundwater table below the sliding surface (i.e. for a drained sliding mass condition). They obtained the lowest factors of safety (FS), less than unity, for both groundwater conditions using the lower limits of the residual shear strength parameters. The highest FS values were found for the upper limits of the shear strength parameters. However, FS became equal to unity if the mean residual shear strength parameters of the bedding plane and the groundwater table observed in the field are considered. When compared to the FS values obtained from the analyses of the upper and lower values of shear strength parameters ( $c_r$ ,  $\phi_r$ ), the FS of the slope ranges between the values above and below unity depending on the variations in shear strength of the bedding and depth of the groundwater table. These results may explain why a catastrophic failure has not occurred yet. These analyses also indicated that a groundwater table at a depth of 7 m from the surface would allow a limiting equilibrium condition (FS = 1). However, such a critical situation can be easily disturbed by seismic loads with an earthquake causing ground motions less than 0.05 g, which may be caused by an earthquake with a magnitude of 4.0. Considering earthquakes since 1940, there are many earthquakes with a magnitude greater than 5 (Çelik 2012). Therefore, Gündoğdu district should have failed and ended up in the Gökdere stream if the critical condition suggested by Çevik and Ulusay (2005) should have been valid. In other words, the limit equilibrium method is not applicable to the situation in Gündoğdu creep-like mass movement and a different approach must be introduced as explained in the next sub-section.

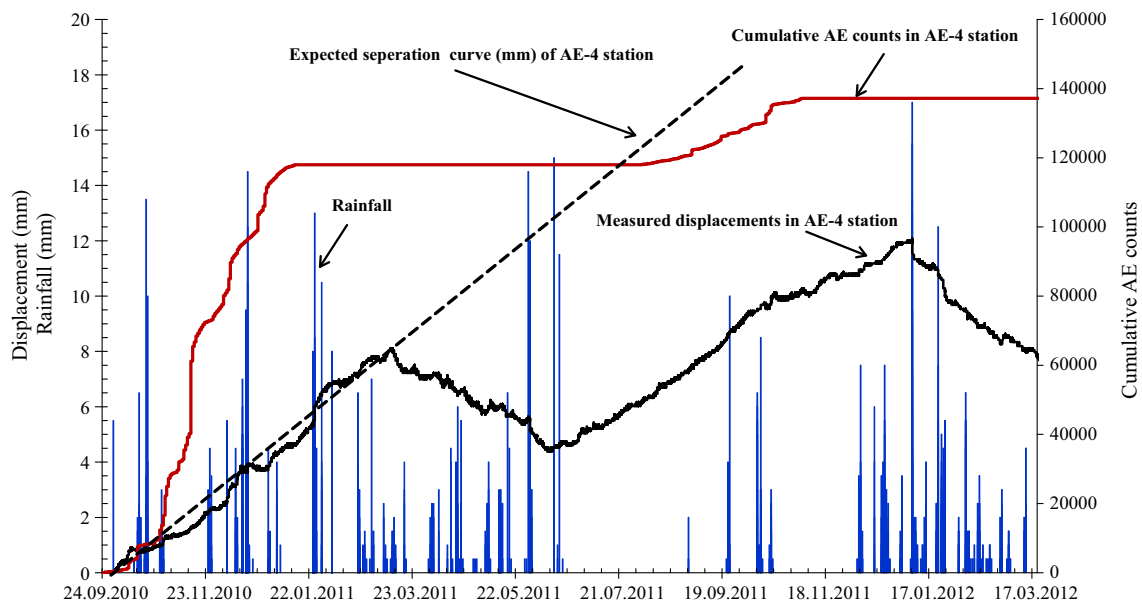


Fig. 16 Comparison of AE counts, gap measurements and rainfall data monitored at station AE4 (after Çelik 2012)

**7.2 Analysis of Creep-like Deformation Using Modified Discrete Finite Element Method**

As noted from Figs. 15 and 16, the deformation response of the unstable body is closely related to rainfall data. In other words, the rainfall results in the variation of cyclic saturation and drying of a zone above a stationary continuously saturated zone. Figure 19a shows the relation between the amount of rainfall ( $h_{RF}$ ) and variation in groundwater level ( $\Delta h_w$ ). The data shown in Fig. 19a can be fitted to the following empirical relation:

$$\Delta h_w = 2.18 h_{RF}. \tag{1}$$

Although the observation data is quite scattered around the fitted line, it should serve for the approach to be adopted in this section.

It is also well known that deformability and strength characteristics of rocks containing minerals or particles, which are prone to absorb water, vary with water content of the rock environment. When saturation increases, their stiffness and strength decrease, while the opposite behaviour is observed upon desorption. The authors carried out some experiments on marl samples with different water contents and they found that such variations do occur upon cyclic saturation and drying. Figure 19b shows the results of the direct shear experiments on marl samples, which are quite relevant to the problem in hand. As noted from Fig. 19b, the shear stiffness and shear strength of marl decreases upon saturation. Some experiments were also carried out by terminating the shearing and letting the sample to dry and to see how the shear stiffness recovers. The experiments revealed that the shear stiffness recovers

to its almost original value upon drying. However, the sample does not recover from its original configuration. This situation may be visualised as illustrated in Fig. 20. A series of theoretical and one-dimensional finite element analyses were first carried out by considering a semi-infinite layer subjected to variations of shear modulus on an incline (Aydan 1994) and its validity was confirmed. The constitutive model shown in Fig. 20 was considered in the numerical scheme and was adopted in this study. It is assumed that a zone with a thickness related to groundwater variation is subjected to cyclic saturation and drying, whose shear stiffness obeys the constitutive law shown in Fig. 20.

If the stress variations take at slow rates, the equation of motion without inertial term may be used in incremental form as given below:

$$\nabla \cdot \dot{\sigma} = 0. \tag{2}$$

The simplest constitutive law for rock between stress and strain fields would be a linear law, in which the properties of rocks may be related to the water content ( $\theta$ ) in the following form (Aydan and Ulusay 2003; Aydan et al. 2006).

$$\dot{\sigma} = D(\theta) \dot{\epsilon}_e. \tag{3}$$

It should be noted that it is necessary to evaluate the non-linear behaviour in an analogy to elasto-plastic analyses if a constitutive law given by Eq. (3) is employed. The volumetric strain variations associated with swelling (inversely shrinkage) may be related to the strain field in the following form:

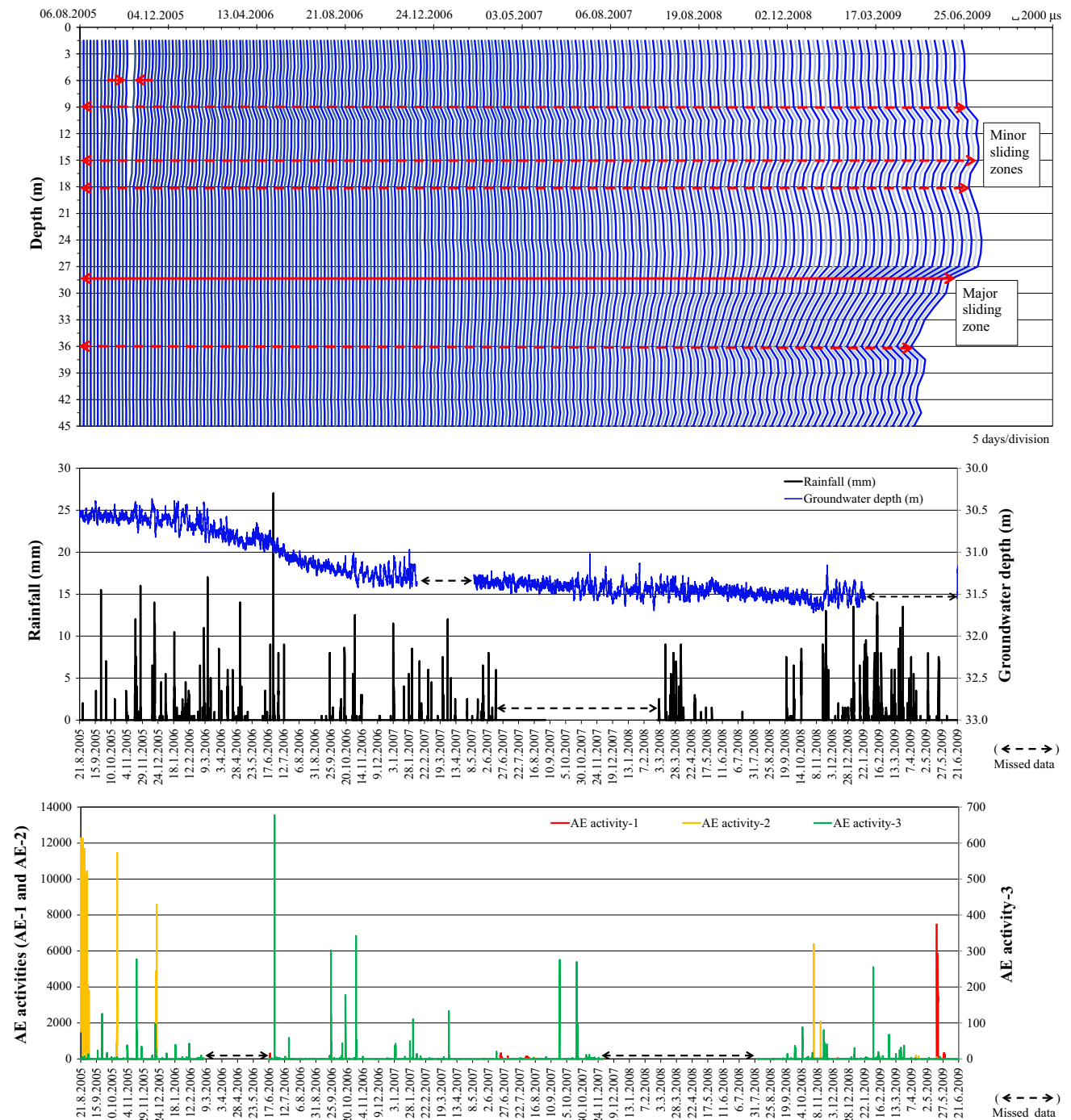


**Fig. 17** Relation between AE numbers, groundwater, rainfall and pipe strain data during the monitoring period between 21 August 2005 and 21 June 2009

$$\dot{\epsilon}_e = \dot{\epsilon} - \dot{\epsilon}_s \tag{4}$$

The finite element form of incremental equation of motion given by Eq. (2) can be shown to be as follows:

$$[K]\{\dot{U}\} = \{\dot{F}\}, \tag{5}$$

where

$$[K] = \int_V [B]^T [D] [B] dV, \tag{6}$$

$$\{\dot{F}\} = \int_V [B]^T [D] \{\dot{\epsilon}_s\} dV + \int_S [\bar{N}]^T \{t\} dS.$$

The discrete finite element method (DFEM) (e.g. Aydan et al. 1996b; Mamaghani and Aydan 1999) was modified in



**Table 2** Physical and mechanical properties of sandstone and marl (Kumsar et al. 2004)

Rock type	Unit weight (kN/m <sup>3</sup> )	Porosity (%)	P-wave velocity, $V_p$ (km/s)	Uniaxial compressive strength (MPa)	Needle penetration index, NPI (N/mm)
Sandstone	17.7–18.2	18.9–25.8	0.8–1.2	0.25–0.6	7.06
Yellowish marl	14.1–14.9	–	1.3–1.8	3.4–6.5	2.86
Reddish marl	16.8–17.9	–	1.1–1.7	8.3–8.5	
Green Marl	15.7–16.9	–	1.3–2.1	–	2.86

**Table 3** Shear strength parameters of marl samples tested under 0.5 mm/min shearing velocity and drained condition (Kumsar et al. 2015)

Type of marl	Water content (%)	Peak cohesion $c_p$ (kPa)	Peak internal friction angle $\phi_p$ (°)	Residual cohesion $c_r$ (kPa)	Residual internal friction angle $\phi_r$ (°)	Natural unit weight $\gamma_n$ (kN/m <sup>3</sup> )	Dry unit weight $\gamma_d$ (kN/m <sup>3</sup> )
Yellowish marl	23	72.5	18.77	56.5	17.74	17.0	13.7
Reddish marl	24	32.5	25.64	30.5	24.23	19.7	14.8

**Table 4** Shear strength parameters of the interlayer between the sandstone and marl under different shearing rates

Shearing rate (mm/min)	Peak cohesion, $c_p$ (kPa)	Peak friction angle, $\phi_p$ (°)	Residual cohesion, $c_r$ (kPa)	Residual friction angle, $\phi_r$ (°)	Tested by
0.25 (wet*)	6.8	24.2	3.54	23.8	Çevik (2003)
0.08 (wet*)	2.6	21.2	1.01	20.9	Çevik (2003)
0.035 (wet*)	2.9	11.2	0.59	10.8	Çevik (2003)
0.5 (wet*)	10.2	27.0	9.40	26.3	Çelik (2012)

wet\* water was injected into interlayer between sandstone and marl during shearing

**Table 5** Friction properties of bedding planes determined from tilt tests in Gündoğdu area (Aydan 2003)

Sample type	Friction angle, $\phi$ (°)
Sandstone–sandstone dry interface tilting test in Laboratory	33–38
Sandstone–sandstone wet interface tilting test in Laboratory	38–43
Marl–sandstone dry interface tilting test in Laboratory	32–40
Marl–sandstone wet interface tilting test in Laboratory	30–47
Marl–marl dry interface tilting test in Laboratory	40–43
Marl–marl wet interface tilting test in Laboratory	31–46
Marl–sandstone dry interface tilting test in situ	32–36
Sandstone–sandstone wet interface tilting test in situ	32

order to take into account the effect of cyclic saturation and drying and it was re-named as DFEM-CSH. In this model, a zone of weakness, whose thickness is associated with the fluctuation of groundwater level, is modelled using the

contact element, while the rest of rock mass is modelled by solid elements. The method is based on updated Lagrangian scheme and it is very easy to implement the variation of the properties of rock mass and zones of weakness.

**Fig. 18** **a** Topographic map of Babadağ and cross-section line along the Gündoğdu landslide, **b** inferred failure surfaces on section A–A’ determined from the pipe strain and surface deformation monitoring data

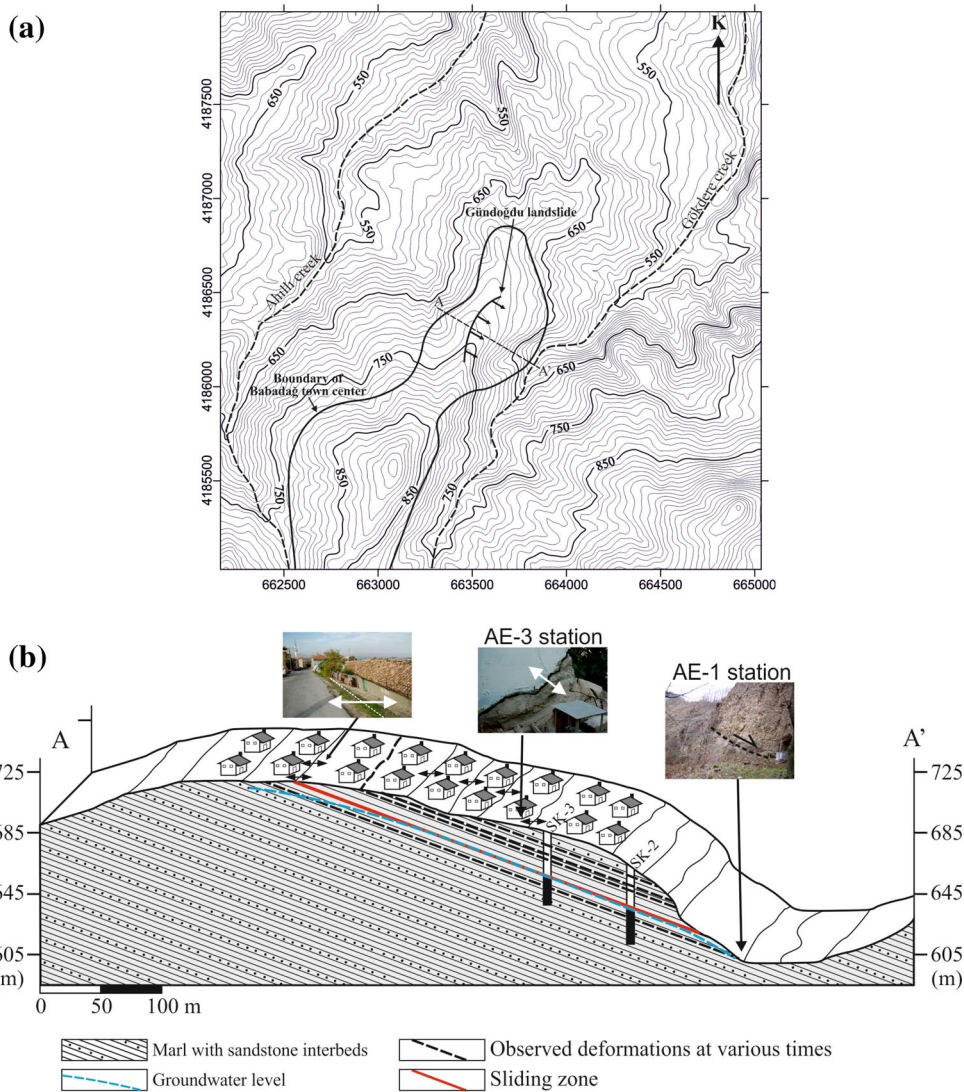
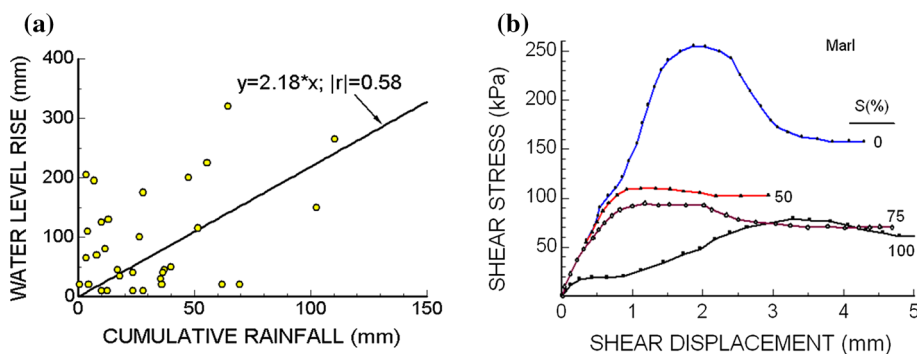


**Fig. 19** **a** Relation between cumulative rainfall and groundwater level, **b** displacement–shear stress responses of marl samples with different saturation conditions under a normal stress level of 245 kPa



The zone of weakness was assumed to coincide with that used in the classical limiting equilibrium methods of analysis. The material properties given in Table 6 are used in the numerical analyses and a number of different conditions were considered. Figure 21a shows the numerical model and the response of the selected points as a function

of time. The largest displacement occurs in the thickest section of the unstable body. As noted from the figure, the displacements at each point differ and it is not purely a rigid-body-like ground deformation. The maximum ground deformation occurs at the middle top of about 150 mm for about 215 days.

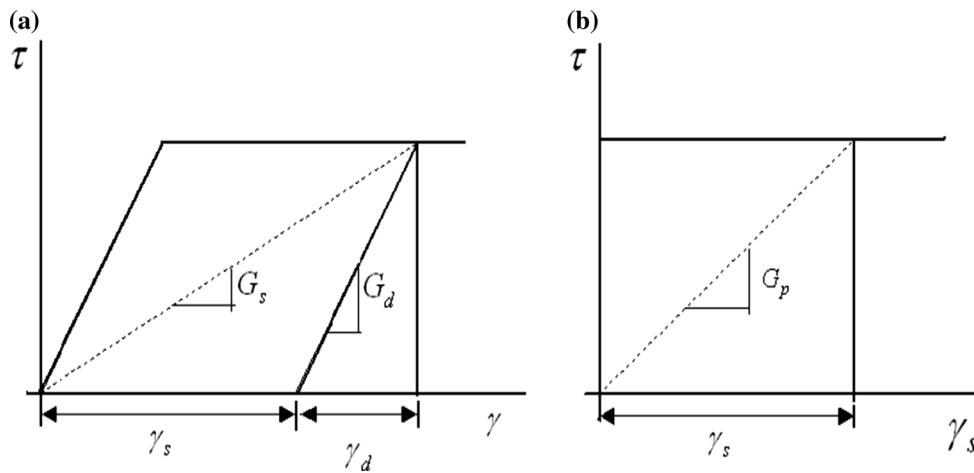


**Fig. 20** Constitutive modelling of cyclic softening-hardening of marl layer

**Table 6** Material properties used in the numerical analyses

Rock	$\lambda$ (MPa)	$\mu$ (MPa)	$\gamma$ (kN/m <sup>3</sup> )	$c$ (kPa)	$\varphi$ (°)	$\sigma_t$ (MPa)
Bottom layer	1000	1000	18.6	5	26.3	1
Top layer	300	300	18.6	5	26.3	1
Contact	300	30	–	0.5	6	0.05

$\lambda, \mu$  Lamé constants,  $\gamma$  unit weight,  $c$  cohesion,  $\varphi$  friction angle,  $\sigma_t$  tensile strength

Figure 21b shows horizontal ground deformation at a given section for different time steps. It is very interesting to notice that the overall ground deformation resembles to those measured from pipe strain gauge in the field shown in Fig. 17. The striking similarity implies that the model developed for the ground deformations in the Gündoğdu district of Babadağ can be properly simulated. This model should probably be the best model so far to explain the creep-like deformation behaviour observed in the study site.

### 8 Evaluation of the Landslide Area in Terms of Natural Hazard

In their project report, Tano et al. (2006a) discussed the preliminary results of the investigations conducted in the Gündoğdu landslide area. The Governor of Denizli Prefecture, the Governor of Babadağ County and the Municipality of Babadağ took the results into account. Four engineers from the Ministry of Public Affairs and Settlement of Turkey visited Babadağ and surveyed the stability problems in the Gündoğdu district. In the report by Şeren et al. (2006), it was stated that there were 436 houses, 111 working shops and ateliers and 19 official buildings affected by the creep-like landslide in the Gündoğdu district. It was also indicated that the lives of the people living in this district were in danger due to the presence of the considerably damaged buildings. Finally, it was

recommended that the landslide area should be restricted to settlement and the all people living there should be evacuated to a safer place.

The Construction Ministry of Turkish Republic accepted and announced that the Babadağ Gündoğdu district would be considered as an Area Subjected to Natural Disaster according to the second article of No. 7269 law. A meeting with local people was organised in Babadağ by the Construction Ministry of Turkish Republic, the project team and other related authorities on the basis of the suggestions of the reports prepared by Tano et al. (2006a) and Şener et al. (2006). Since the old people used this unstable area to live there throughout most of their life, the local people exhibited a resistant in this first meeting. However, they were convinced to leave their damaged houses after several follow-up meetings.

A new settlement area, called Kayalar District, 10 km northeast of Denizli city centre, was selected by the Disaster and Emergency Management Authority of Turkey, and new houses, workshops and ateliers were built for the people of the Gündoğdu district (Fig. 22a–c), and finally, they moved to their new houses in March 2012.

The houses were demolished (Fig. 22d, e) after the people moved from the Gündoğdu landslide area in Babadağ, according to the regulations written in the second article of No. 7269 numbered law. The authors suggested that this area should be used as a geopark area to show the effects of a creep-like landslide to people for focusing their attention on future planning of cities and towns.

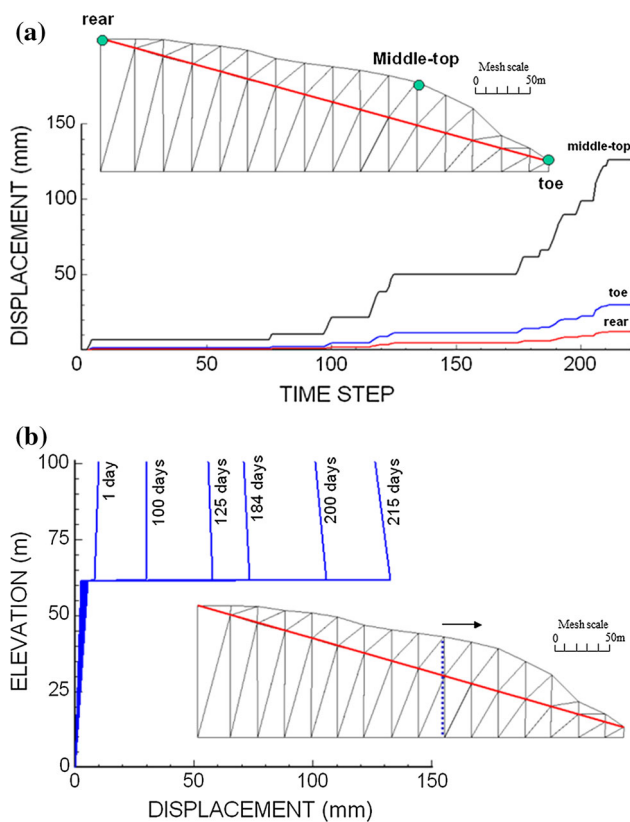


**Fig. 21** **a** Displacement responses of three selected points in the analysed domain, **b** ground deformation at a given section for different time steps

## 9 Conclusions

A creep-like landslide has negatively affected the life of people living in the Gündoğdu district of Babadağ town for more than seventy years. The authors presented an integrated study of geomechanical investigations and laboratory and in situ tests, continuous in situ monitoring and analytical and numerical models to explain the ground deformation behaviour observed at the Gündoğdu district of Babadağ for decades.

Babadağ sandstone-marl succession forms the Gündoğdu landslide area and the stratification dips towards SE to a stream valley. The unfavourable orientation of the geological structure with respect to the slope and their low geomechanical properties and the rock units of the slope in this district play an important role on the creep-like movements.

Since the Babadağ people used to earn their income mainly from the textile production by means of vibrating weaving machines, in situ acceleration measurements were taken during their operation. The results showed that machinery vibrations may have a slight dynamic effect on

the stability of the slope. However, it is extremely difficult to differentiate this effect from those of all other factors.

In situ infiltration test results indicate that rain water infiltrates into the slope quickly and influences groundwater variation. The overall deformation rates by aerial photogrammetry measurements range between 40 and 160 mm/year, which are quite consistent with the relative displacement measurements using a laser metre.

The monitoring data of pipe strain, groundwater level fluctuation, rainfall, and AE data showed that slope failure accelerated during and after rainy seasons. Slope movements have been taking place along the sandstone-marl bedding planes at 5 different levels from the ground surface as inferred from the monitored data of the pipe strain in location of borehole SK3. Minor deformations were observed at 9, 15, 18 and 36 m. The major mass movement was recorded at the level of 29 m.

Classical approaches incorporating sliding surface in limiting equilibrium methods or numerical techniques cannot be precisely used to simulate the step-like deformations. However, such approaches can only simulate very short durations, say in several seconds or hours, and they can not explain the deformations for decades. Probably visco-plastic approaches may be used for this purpose. But they will not yield step-like ground deformation as observed in situ. In general, a coupled approach is necessary to model ground deformations in the Gündoğdu district of Babadağ. However, if the continuous groundwater fluctuation data are available as in the case of the Gündoğdu district, the analytical and numerical models presented in this study are capable of what is observed in situ. From the presented results of simulations and comparisons with measured responses, it can be concluded that the model developed in this study should probably be the best model so far to explain the observed deformation behaviour in the Gündoğdu district of Babadağ.

The Denizli basin is located in an earthquake prone area. The region can face very large earthquakes in due time. Magnitudes of earthquakes bigger than 6 in the close vicinity of Babadağ (i.e. Babadağ fault) may cause very large mass movements in the Gündoğdu district resulting in its total failure (Çelik et al. 2012; Aydan and Kumsar 2014; Kumsar and Aydan 2007).

On the basis of the results from this long-term project, the Construction Ministry of Turkish Republic designated the Gündoğdu district as “An Area Subjected to Natural Disaster”. After this declaration, a new settlement place for the people living in the district was selected where their new houses, workshops and ateliers were built, and then the people moved there since 2012.

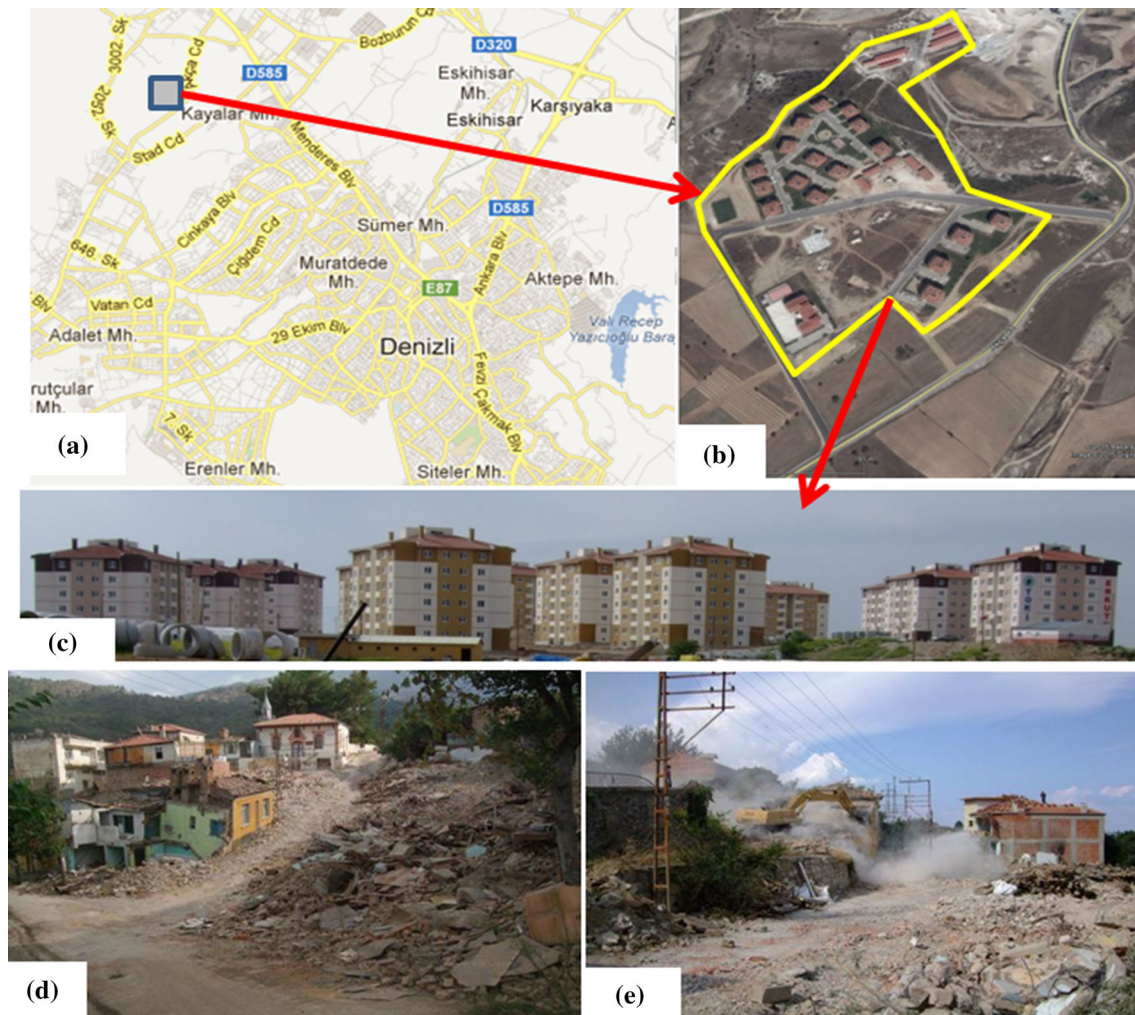


**Fig. 22** a–c Location of the new settlement area and the apartments for the people of Gündoğdu district, d–e views from the demolished houses after Gündoğdu district was evacuated

This integrated study of geotechnical investigations, laboratory and in situ tests, continuous multi-parameter monitoring and analytical and numerical analyses based on the principles of rock mechanics and rock engineering is one of the successful applications of preventing the disastrous effects of rock slope failures on people before a catastrophic event with the collaboration of authorities in national and local levels. By virtue of this integrated study, the people of the Gündoğdu district of Babadağ now live in a safe area.

**Acknowledgments** The authors would like to thank to Japanese Ministry of Education and Culture for supporting the research project named as Collaborative Research on the Geo-environmental Factors on Slope Movements and the Investigation of Creeping Slope Movements at Babadağ town, Turkey as a Case Study, and Pamukkale University Scientific Research Department for supporting research projects with the numbers of 2005FBE007 and 2009KRM001. The authors also thank to the Governor of Denizli City, Governor of Babadağ town, Municipality of

Babadağ, Department of Environment and Public Works of Denizli, Disaster and Emergency Management Department of Denizli and Mustafa Kaya (Geological Engineer) for their kind support to the project.

## References

- Atak O, Aksu O, Aydan Ö, Çevik Y (2003) The evaluation of long-term ground deformation of the landslide area of Babadağ through aerial photogrammetry technique. An International Colloquium on the Instrumentation and Monitoring of Landslides and Earthquakes in Japan and Turkey, Koriyama, Japan, pp 133–142
- Aydan Ö (1994) The dynamic shear response of an infinitely long visco-elastic layer under gravitational loading. *Soil Dyn Earthq Eng* 13:181–186
- Aydan Ö (1997) The seismic characteristics of and the occurrence pattern of Turkish earthquakes. Turkish Earthquake Foundation, Report No: TDV/TR 97-007, İstanbul
- Aydan Ö (1998) Finite element analysis of transient pulse method test for permeability measurements. The 4th European Conference

- on Numerical Methods in Geotechnical Engineering- NUMGE98, Udine, pp 719–727
- Aydan Ö (2003) The mechanism of the long-term landslide at Babadağ. An International Colloquium on The Instrumentation and Monitoring of Landslides and Earthquakes in Japan and Turkey, Koriyama, Japan, pp 39–50
- Aydan Ö, Kumsar H (2005) Some observations of the seismic damage to antique cities and structures in Denizli region. In: Özkul M, Yağız S, Jones B (eds) Proceedings of the 1st international symposium on travertine, September 21–25, Denizli, Turkey, pp 211–216
- Aydan Ö, Kumsar H (2014) Assessment of the earthquake potential of the west Aegean region of Turkey based on seismicity, tectonics, crustal deformation and geo-archaeological evidence and its geotechnical aspects. Bull Eng Geol Environ. doi:10.1007/s10064-014-0684-7
- Aydan Ö, Ulusay R (2003) Geotechnical and geoenvironmental characteristics of man-made underground structures in Cappadocia, Turkey. Eng Geol 69:245–272
- Aydan Ö, Shimizu Y, Ichikawa Y (1989) The effective failure modes and stability of slopes in rock mass with two discontinuity sets. Rock Mech Rock Eng 22(3):163–188
- Aydan Ö, Sezaki M, Yarar R (1996a) The seismic characteristics of Turkish earthquakes. Eleventh World Conference on Earthquake Engineering, Acapulco, Mexico
- Aydan Ö, Mamaghani IHP, Kawamoto T (1996b) Application of discrete finite element method (DFEM) to rock engineering structures, Proceedings of NARMS'96, pp 2039–2046
- Aydan Ö, Kumsar H, Ulusay R, Shimizu Y (1997) Assessing limiting equilibrium methods (LEM) for slope stability by discrete finite element method (DFEM). IACMAG, Wuhan, pp 1681–1686
- Aydan Ö, Ulusay R, Kumsar H (2002) How to infer the possible mechanism and characteristics of earthquakes from the striations and ground surface traces of existing faults. Struct Earthq Eng (J Japan Soc Civil Eng) 19(2):199–208
- Aydan Ö, Ulusay R, Kumsar H, Çevik Y (2003) Laboratory and in situ tests on rocks and bedding planes and machinery induced vibrations of Babadağ landslide area. An International Colloquium on the Instrumentation and Monitoring of Landslides and Earthquakes in Japan and Turkey, Koriyama, Japan, pp 91–100
- Aydan Ö, Daido M, Tano H, Nakama S, Matsui H (2006) The failure mechanism of around horizontal boreholes excavated in sedimentary rock. 50th US Rock Mechanics Symposium, Paper No. 06-130
- Barron K, Hedley DGE, Coates DF (1970) Field instrumentation for rock slopes. Proceedings of the 1st international conference on stability in open pit mining, Vancouver, Canada, pp 143–168
- Çelik SB (2012) Investigation of the slope instability in Babadağ town (Denizli) using multi parameter monitoring techniques, physical model tests and mathematical methods. PhD dissertation, Pamukkale University, Denizli (in Turkish)
- Çelik SB, Kumsar H, Aydan Ö (2011). The investigation of the mechanism of Babadağ Gündoğdu landslide through static and dynamic physical model tests, ROCMEC'2011-Xth Regional Rock Mechanics Symposium, Ankara, Turkey, pp 196–170 (in Turkish)
- Çevik SY (2003) An investigation on the causes, mechanism and modelling of slope instability at Babadağ town (Denizli). MSc dissertation, Hacettepe University (in Turkish)
- Çevik YS, Ulusay R (2003) An overview of Babadağ (Turkey) landslide. Proc. International Colloquium on the Instrumentation and Monitoring of Landslides and Earthquakes in Japan and Turkey, Koriyama, Japan, pp 17–26
- Çevik SY, Ulusay R (2005) Engineering geological assessments of the repeated plane shear slope instability threatening Babadağ (Turkey) and its environmental impacts. Environ Geol 47:685–701
- Ergin K, Güçlü U, Uz Z (1967) A catalogue of earthquakes for Turkey and surrounding area. ITU, Faculty of Mining Engineering, No. 24 (in Turkish)
- Ergün M (1969) Geological investigation report. The Construction Ministry of Turkish Republic, Investigation and Planning Department of General Directorate of Natural Disaster Affairs, Ankara (in Turkish)
- Eyidoğan H, Güçlü U, Utku Z, Değirmenci E (1991) Macro-seismic catalogues of large Turkish earthquakes (1900–1988). ITU, Faculty of Mines, İstanbul (in Turkish)
- Hançer M (2013) Study of the structural evolution of the Babadağ-Honaz and Pamukkale Fault zones and the related earthquake risk potential of the Buldan region in SW Anatolia, East of the Mediterranean. J Earth Sci 24(3):397–409
- Hoek E, Bray JW (1981) Rock slope engineering. Institution of Mining and Metallurgy, Revised 3rd edn, London
- ISRM (2007) The complete ISRM suggested methods for rock characterization, testing and monitoring: 1974–2006. In: Ulusay R, Hudson JA (eds) Suggested methods prepared by the commission on testing methods, International Society for Rock Mechanics, Compilation Arranged by the ISRM Turkish National Group, Ankara, Turkey
- KOERI (2014) <http://www.koeri.boun.edu.tr/scripts/1st4.asp>
- Kumsar H (1993) Computerized mine slope stability assessment by using inter-slice force transmission theory. PhD Dissertation, Nottingham University, UK
- Kumsar H, Aydan Ö (2007) Faulting and shaking characteristics of earthquakes in Denizli province (Turkey). In: Nakoman ME, İnaner H, Tanyer NU (eds) Int Earth Science Colloquium on the Egean Region, IESCA 2005, Dokuz Eylül University, İzmir, pp 231–241
- Kumsar H, Aydan Ö, Ulusay R (2000) Dynamic and static assessment for rock slopes against wedge failures. Rock Mech Rock Eng 33(1):31–52
- Kumsar H, Aydan Ö, Tano H, Atak O (2004) An investigation of a long-term landslide of Babadağ (Denizli) from a rock mechanics point of view. ROCKMEC'2004-VIIIth Regional Rock Mechanics Symposium, 2004, Sivas, Turkey, pp 277–287 (in Turkish)
- Kumsar H, Aydan Ö, Tano H, Çelik SB (2008) Engineering investigation on the July 2008 Buldan (Denizli) Earthquakes. Ekin Press, Bursa (in Turkish)
- Kumsar H, Çelik SB, Aydan Ö, Tano H, Ulusay R (2012) Investigation of Babadağ Gündoğdu landslide by using multi-parameter monitoring techniques and its evaluation within natural hazard scope. 65th Year Mahir Vardar geomechanic, tunneling and rock structures symposium, İstanbul, pp 311–337 (in Turkish)
- Kumsar H, Aydan Ö, Korkmaz B, Çalık, T, Işıkan B, Ercan F (2015) Occurrence mechanism and investigation of north Delikir hill landslide (Denizli-Babadağ), Turkish Geological Congress, 2015, Ankara, Abstract book (in Turkish), pp 428–429
- Mamaghani IHP, Aydan Ö (1999) Analysis of masonry structures under dynamic and static loading by discrete finite element method. JSCE Struct Eng Earthq Eng 16(2):1–12
- MTA (2014) <http://yerbilimleri.mta.gov.tr/anasayfa.aspx>
- Önay TS (1946) Landslides in the vicinity of Babadağ. Bull Miner Res Explor 36:300–304 (in Turkish)
- Öngür T (1971) Geological investigation and geothermal potential of Denizli-Babadağ and surrounding. MTA Report No: 4689, Ankara (in Turkish)
- Özpinar Y, Köseoğlu M, Çobanoğlu İ, Ok R, Sabaz Ü (1999a) Mass movements and their classification around Babadağ (Denizli)

- and its surrounding. 1st symposium on Babadağ, Pamukkale University, pp 24–38 **(in Turkish)**
- Özpınar Y, Köseoğlu M, Çobanoğlu İ, Ok R (1999b) Gündoğdu landslide of Babadağ (Denizli) town center. 1st Symposium on Babadağ, Pamukkale University, pp 39–50 **(in Turkish)**
- Şaroğlu F, Emre Ö, Kuşcu İ (1992) Active fault map of Turkey. Publication of Mineral Research and Exploration (MTA) Institute, Ankara **(in Turkish)**
- Şeren İ, Altaylı K, İleri HN, Yılmaz S (2006) Geological investigation report of Babadağ-Gündoğdu district. Ministry of Housing and Settlement, General Directorate of Disaster Affairs, Ankara, **(in Turkish)**
- Şimşek Ş (1984) Geology and geothermal energy possibilities of the area between Denizli-Kızıldere-Tekkehamam-Tosunlar-Buldan-Yenice. Publication of Mineral Research and Exploration (MTA) Institute, Scientific Report No: 7846, Ankara **(in Turkish)**
- Tano H, Kumsar H, Aydan Ö, Ulusay R (2003) The assessment of the Babadağ landslide behavior by a simple field measurement system. An International Colloquium on the Instrumentation and Monitoring of Landslides and Earthquakes in Japan and Turkey, Koriyama, Japan, pp 1–9
- Tano H, Aydan Ö, Ulusay R, Kumsar H (2006a) Joint research related to the effects of geo-environmental factors on slope movements: Investigation of the creep type Babadağ (Turkey) landslide. Interim report **(in Turkish)**
- Tano H, Abe T, Aydan Ö, Kumsar H, Kaya M, Çelik SB, Ulusay R (2006b) Long-term monitoring of Babadağ landslide through an integrated monitoring system with an emphasis on AE responses and ground straining. Symposium on Recent Applications in Engineering Geology, Pamukkale University, Denizli, pp 131–141 **(in Turkish)**
- Tano H, Aydan Ö, Kumsar H, Kaya M, Çelik SB, Ulusay R, Abe T (2008) Investigation of Babadağ landslide and Its implications for hazard mitigation before natural disaster. First Collaborative Symposium of Turk-Japan Civil Engineers, 5 June 2008, İstanbul, pp 65–73